NAVAL POSTGRADUATE SCHOOL
MONTEREY, CALIFORNIA

THESIS

SHIPTRACKS IN THE CALIFORNIAN STRATUS REGION:DEPENDENCY ON MARINE ATMOSPHERIC BOUNDARY LAYER DEPTH

by

Eric J. Trehubenko

December, 1994

Thesis Advisor: Philip A. Durkee

19950411 014

REPORT DOCUMENTATION PAGE

Form Approved OMB No. 0704-0188

1. AGENCY USE ONLY *(Leave blank)*	2. REPORT DATE December 1994	3. REPORT TYPE AND DATES COVERED Master's Thesis

4. TITLE AND SUBTITLE SHIPTRACKS IN THE CALIFORNIAN STRATUS REGION: DEPENDENCY ON MARINE ATMOSPHERIC BOUNDARY LAYER DEPTH	5. FUNDING NUMBERS
6. AUTHOR(S) Eric J. Trehubenko	
7. PERFORMING ORGANIZATION NAME(S) AND ADDRESS(ES) Naval Postgraduate School Monterey CA 93943-5000	8. PERFORMING ORGANIZATION REPORT NUMBER
9. SPONSORING/MONITORING AGENCY NAME(S) AND ADDRESS(ES)	10. SPONSORING/MONITORING AGENCY REPORT NUMBER

11. SUPPLEMENTARY NOTES The views expressed in this thesis are those of the author and do not reflect the official policy or position of the Department of Defense or the U.S. Government.

12a. DISTRIBUTION/AVAILABILITY STATEMENT Approved for public release; distribution is unlimited.	12b. DISTRIBUTION CODE

13. ABSTRACT *(maximum 200 words)*

Analysis of AVHRR (Advanced Very High Resolution Radiometer) satellite image/atmospheric sounding pairs reveals that the development and persistence of shiptracks is dependent on Marine Atmospheric Boundary Layer Depth (MABL). 65 image/sounding pairs were analyzed with eight cases featured. The data was collected from the SEAHUNT (July 1991) and MAST (June 1994) field experiments off the western coast of the United States. A distribution of cloud-topped MABLs for the dataset reveals that shiptracks developed in boundary layers of depth less than 750 meters. A mean number of shiptracks versus MABL depth reveals that shiptracks decrease in number with increasing boundary layer depth, supporting MAST hypotheses. Several mechanisms are proposed to explain the decrease in track development with increasing MABL depth and these present several avenues for future data analyses. Additionally, a composite track environment is also presented to document other environmental variables encountered during the analysis deemed pertinent to shiptrack formation.

14. SUBJECT TERMS shiptrack, boundary layer depth, stratiform, AVHRR	15. NUMBER OF PAGES 101
	16. PRICE CODE

17. SECURITY CLASSIFICATION OF REPORT Unclassified	18. SECURITY CLASSIFICATION OF THIS PAGE Unclassified	19. SECURITY CLASSIFICATION OF ABSTRACT Unclassified	20. LIMITATION OF ABSTRACT UL

NSN 7540-01-280-5500

Standard Form 298 (Rev. 2-89)
Prescribed by ANSI Std. 239-18 298-102

i

SHIPTRACKS IN THE CALIFORNIAN STRATUS REGION: DEPENDENCY ON MARINE ATMOSPHERIC BOUNDARY LAYER DEPTH

by

Eric J. Trehubenko
Lieutenant, United States Navy
B.A., Boston University, 1988

Submitted in partial fulfillment
of the requirements for the degree of

MASTER OF SCIENCE IN METEOROLOGY AND PHYSICAL OCEANOGRAPHY

from the

NAVAL POSTGRADUATE SCHOOL
December 1994

Author: _____

Eric J. Trehubenko

Approved by: _____

Philip A. Durkee, Thesis Advisor

_____

Kenneth L. Davidson, Second Reader

_____

Robert L. Haney, Chairman
Department of Meteorology

iii

Accesion For		
NTIS CRA&I		☒
DTIC TAB		☐
Unannounced		☐
Justification		
By _____		
Distribution /		
Availability Codes		
Dist	Avail and / or Special	
A-1		

ABSTRACT

Analysis of AVHRR (Advanced Very High Resolution Radiometer) satellite image/atmospheric sounding pairs reveals that the development and persistence of shiptracks is dependent on Marine Atmospheric Boundary Layer Depth (MABL). 65 image/sounding pairs were analyzed with eight cases featured. The data was collected from the SEAHUNT (July 1991) and MAST (June 1994) field experiments off the western coast of the United States. A distribution of cloud-topped MABLs for the dataset reveals that shiptracks developed in boundary layers of depth less than 750 meters. A mean number of shiptracks versus MABL depth reveals that shiptracks decrease in number with increasing boundary layer depth, supporting MAST hypotheses. Several mechanisms are proposed to explain the decrease in track development with increasing MABL depth and these present several avenues for future data analyses. Additionally, a composite track environment is also presented to document other environmental variables encountered during the analysis deemed pertinent to shiptrack formation.

TABLE OF CONTENTS

ix

ACKNOWLEDGEMENTS

A number of individuals contributed greatly to the completion of this thesis. Professors Phil Durkee and Ken Davidson provided continuous guidance and encouragement and kept me "on the path". Thank you, gentlemen. Also, many thanks are owed to the support staff in both the Meteorology and Oceanography departments. Mary Jordan was instrumental in my converting the sounding data files to "GEMPAK-friendly" format and Mike Cook's unparalleled command of MATLAB no doubt saved me from many hours of frustration. Kurt Nielsen and Chuck Skupniewicz introduced me to the world of TERASCAN and developed several programs that allowed for a much faster processing of the HRPT data, tailored to my needs. Without their help, this project would not have been the success that it has become.

Finally, I would like to thank my wife, Emily and my sons John and Andrew for their constant love and support. This thesis is dedicated to them.

I. INTRODUCTION

Shiptracks have been observed in satellite images for nearly three decades. Even in the earliest images, these "anomalous cloud lines" were suspected to have been caused by the addition of aerosol particles to the marine environment by ships (Conover, 1966; Twomey, 1968).

Our increasing ability to detect shiptracks and the ships producing them has prompted interest in understanding the processes by which these tracks are formed. An obvious motivation for understanding the physical processes behind shiptrack development is a desire to develop a capability to predict their formation, as well as possibly prevent their occurrence. A less obvious, but more fundamental motivation is to understand how anthropogenic aerosols modify the reflectivity of clouds, and thus the earth's radiation balance. The perturbation of cloud albedo by anthropogenic aerosols is an indirect radiative effect which may have important consequences in terms of global climate (Charlson,1987; Charlson, 1992; Albrecht, 1989).

Not every ship causes a shiptrack. Shiptracks are seldom (if ever) observed in some geographical locations, while they are prevalent in others. Clearly, there must be a combination of ambient conditions necessary in the marine atmosphere before shiptracks will form. Conover (1966) and Bowley (1967) suggested several conditions from early observations from TIROS satellites. The conditions suggested were 1) A shallow, cloud-topped, well-mixed boundary layer; 2) A low number of cloud condensation nuclei (CCN); and 3) A relatively narrow range of temperatures and relative humidities at the surface.

Conover's list may not be exhaustive. There may well be other important conditions necessary for shiptrack formation. Therefore, a detailed knowledge of background conditions is necessary for the situations when shiptracks form, as well as in the situations when they do not.

1

This thesis represents an effort to better define the background environmental parameters associated with shiptrack development. Of primary concern is the influence of marine boundary layer depth on the occurrence or non-occurrence of shiptracks.

Chapter II of this thesis, *Background*, discusses previous observations of shiptracks and the environments in which they have been observed. Additionally, descriptions of two field experiments designed specifically to investigate the shiptrack phenomenon are described. Specific hypotheses from these experiments pertinent to this thesis are presented and the data used from them is described. Chapter III, *Methodology*, describes how the data was processed and what assumptions were made during the analysis. Chapter IV, *Analysis/Results*, presents several case studies in which shiptracks were observed and not observed. Additional comments on cases not specifically featured in the thesis are also provided. A composite dataset from both experiments is created and analyzed, revealing dependency of shiptrack development and persistence on the depth of the marine boundary layer. Mechanisms proposed to explain this observed phenomenon are also presented. Finally, conclusions from this study and recommendations for future work are presented in Chapter V, *Conclusions and Recommendations*.

II. BACKGROUND

A. PREVIOUS SHIPTRACK STUDIES

1. Image Analysis

Nearly three decades ago, Conover (1966) noted that under some circumstances, ships can disturb the marine atmospheric boundary layer, generating what he termed "anomalous cloud lines". These cloud lines could be detected in the visible wavelengths of TIROS VII satellite images as long, narrow, linear clouds. More recently, it has been noted that ship effects are more frequently observed in the wavelengths of the near-infrared (near-IR) as modifications to preexisting marine stratus clouds. These "shiptracks" are not the same phenomenon as the cloud lines mentioned above in that they are a result of the modification of existing clouds vice a cloud generation mechanism. It is probable that these two mechanism are related.

Coakley et al. (1987) first described this near-IR shiptrack signature through satellite observations made with the National Oceanographic and Atmospheric Administration's Advanced Very High Resolution Radiometer (NOAA's AVHRR) onboard that agency's polar orbiting satellites. At 3.7 microns (3.7 μm) (AVHRR Channel 3), these tracks appear as long, narrow, linear features of high albedo embedded in the background cloud and, under suitable environmental conditions, they can extend to several hundred kilometers, lasting for up to two days (Figure 1). It was proposed that emissions from ships could serve as a localized source of cloud condensation nuclei (CCN). In contrast with the low CCN content of the background marine environment, this local region of high CCN could yield an increased number of cloud drops and reduce the average droplet size. At 3.7 μm, the ratio of scattered radiation to absorbed radiation is proportional to r^{-1}, where r is the droplet radius (Coakley et al., 1987). The scattering cross section of a droplet is proportional to its geometric cross section and the absorption cross section is approximately proportional to its volume. Thus the ratio of scattering to
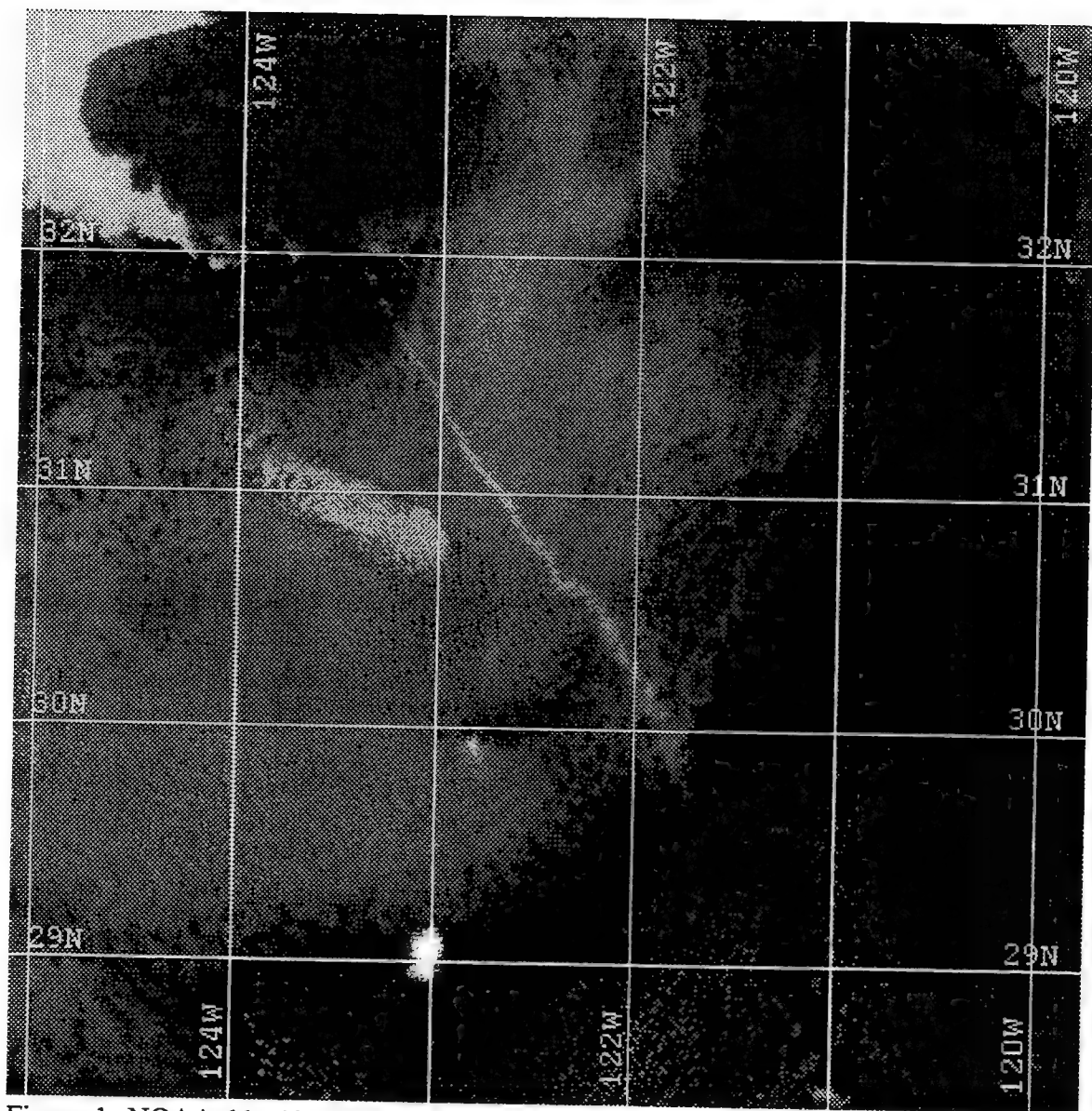
3

Figure 1. NOAA 11, AVHRR Channel 3 image from 13 July 1991, 2209 UTC depicting a shiptrack. Length of this track is over 500 km.

absorption increases as droplet radius decreases, yielding a region of higher albedo at 3.7 µm. As the ship travels and winds advect the plume, the long, linear signature of the shiptrack is produced.

Radke et al. (1989) and King et al. (1990) have presented analyses of measurements from aircraft in ship-influenced cloud. Both studies reveal that cloud microphysical effects are important for the formation of shiptracks. In both reports, it was found that there was an increase in cloud droplet number and decrease in droplet size within the track.

Porch et al. (1990) and Hindman (1990) have expressed the possibility that the marine environment can be affected by a ships passage in ways other than CCN production alone. They suggest that the addition of heat, momentum, and moisture to the environment may also contribute to track production.

Observations indicate that the amount of susceptible cloud cover is the primary contributor to large regions of numerous shiptracks (Figure 2). Platnick and Twomey (1994) have presented calculations of "cloud susceptibility" - the increase in albedo resulting from the addition of one cloud droplet per cubic centimeter (as cloud liquid water content remains constant). Key identified variables in determining cloud susceptibility are cloud optical thickness and droplet size. Marine stratus clouds are expected to be of higher susceptibility since they are cleaner (less CCN per unit volume) than continental clouds. While their results support this, Platnick and Twomey note that susceptibility alone was not a sufficient predictor of tracks.

Image analysis studies have revealed the nature of some of the physical characteristics of shiptracks including width and reflectance (Morehead, 1988; Salvato, 1992; Millman,1992), background environmental characteristics (Pettigrew, 1992; Evans, 1992) and preliminary insight into detection algorithms and occurrence statistics (Lutz, 1992; Giampaolo, 1992; Mays, 1993).

To date, 27 direct correlations of shiptracks and accompanying local weather reports have been made. These include reports of true wind, ship position, speed and
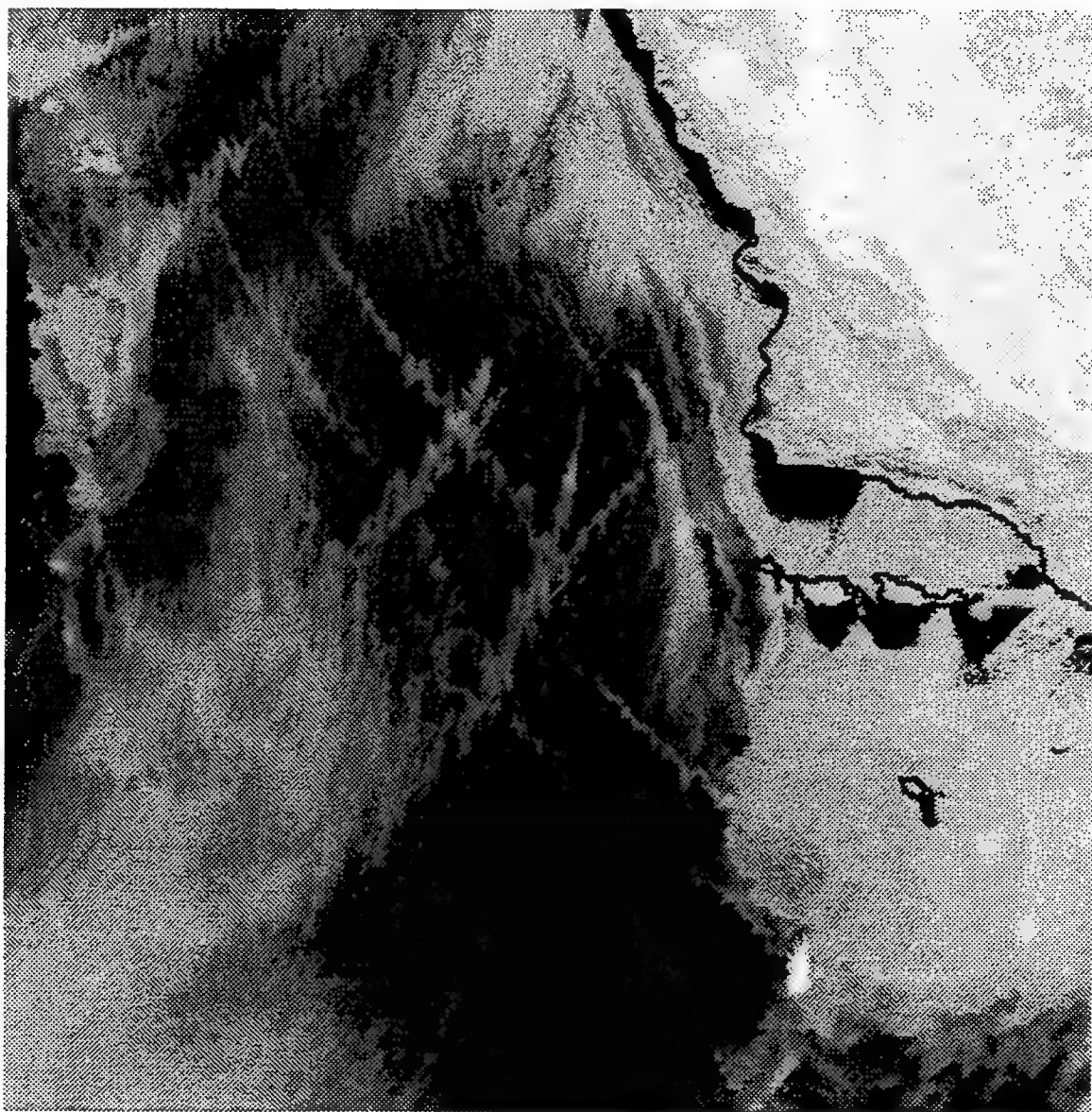
Figure 2. NOAA 11, AVHRR Channel 3 image from 13 July 1991, 2209 UTC depicting a large region of shiptrack-susceptible cloud.

heading (Durkee, 1994). Pettigrew (1992) created a "composite" track environment (Table 1) from weather reports generated by merchant vessels suspected of generating shiptracks. These merchant ship reports have provided some insight, but lack the accuracy required to adequately describe the track-conducive environment.

Shiptracks can form in diverse stratiform cloud types and boundary layer conditions. Evans (1992) and Millman (1993) have indicated that tracks can form in fog, stratus, and stratocumulus cloud regimes with boundary layer depths ranging from very shallow to over one kilometer. Shiptracks have been observed in coupled and decoupled boundary layers. In a coupled boundary layer, the atmosphere is unstable, resulting in vertical motion and mixing throughout the boundary layer. The development of shiptracks in this regime is likely. In a decoupled boundary layer, one in which there is an internal stable layer, mixing in the subcloud region is confined to that regime. It would be expected that the stable transition layer would act to inhibit the transport of ship effluent from the surface to the cloud.

Recent studies of night images (Kuciauskas et al., 1993) indicate that shiptracks appear as long, narrow lines of reduced emittance at 3.7 µm. This reduced emittance is due to the distribution of smaller droplets in the shiptrack relative to the background cloud. At longer wavelengths (11 and 12 µm), clouds emit as black bodies for droplets of all sizes and thus shiptracks do not emit differently than the background cloud and are indiscernible at these wavelengths.

2. Effects of Ship Type

Exactly which ships produce shiptracks is not well understood. It is not clear what conditions must be met for a given ship to produce a track. How tracks are generated based on engine/fuel type or aerosol output is unknown. The current limited database reveals that to date, ships with oil, diesel, steam, and gas turbine propulsion types of various sizes have been correlated to their tracks (Durkee, 1994). Pettigrew (1992) showed trends in the shiptrack database which indicate that steam and oil engine propelled ships have different separation distances from their tracks than diesel propelled ships. A possible hypothesis for this situation is that plume dynamics and CCN concentrations are

7

different for various propulsion systems. It is also conceivable that a shallow boundary layer is more susceptible to modification by effluent from a given ship than a deeper one.

3. In Situ Measurements

In situ measurements of shiptracks and track susceptible environments are quite limited. To date, outside of aircraft flights on designated "ships of opportunity", only two field experiments have been designed with the intent of dedicating assets to make in situ measurements of tracks and the environment in which they develop. Measurements from these two field experiments, Ship-trail Evolution Above High Updraft Naval Targets (SEAHUNT) and the Monterey Area ShipTrack Experiment (MAST) provide the data for this thesis. They will be discussed in greater detail later in this chapter.

B. CLIMATOLOGY

While this thesis concentrates on ship tracks observed in the Californian stratus region (approximately 20°-30°N, 120°-130°W), it should be noted that tracks have been observed in many oceanic regions where stratiform clouds are the type that contribute most to cloud cover. These areas include areas of tactical significance to the Navy, including the Greenland-Iceland-United Kingdom (GIUK) Gap, the eastern North Pacific, and in littoral regions worldwide.

Shiptracks have been noted to occur most often in the stratocumulus clouds that frequently occur on the east side of the oceanic subtropical highs where the trade winds climatologically blow from midlatitudes toward the Inter-Tropical Convergence Zone (ITCZ) (Figure 3). These stratocumulus clouds form over oceans with relatively cold sea surface temperatures (SSTs) and beneath a strong temperature inversion (trade inversion) that caps the boundary layer. This inversion is thought to be maintained by subsidence in the descending branch of the Hadley circulation and limits stratiform convection to the boundary layer (a more detailed description of boundary layer characteristics follows in the next section). As air in the trade winds approaches the ITCZ and warmer water, the trade inversion generally rises and weakens and deeper cumulus convection replaces the stratiform clouds. How cumulus clouds replace stratiform clouds is a question of active
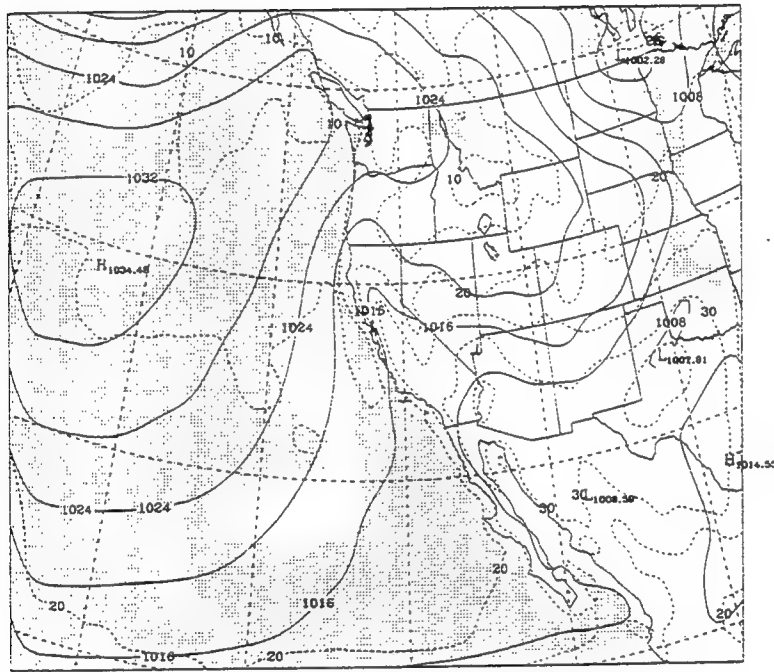
8

slp t rh

Figure 3. Typical synoptic condition in the eastern Pacific associated with shiptrack formation. Shiptracks frequently occur in the stratiform clouds on the east side of oceanic subtropical highs.
(NORAPS model analysis fields: sealevel pressure, temperature, humidity)

research. Subtropical stratocumulus clouds have been studied in great detail through field experiments (e.g., FIRE, off the coast of California in 1987 (Albrecht et al., 1988)), and using a wide variety of models (Klein and Hartmann, 1993).

Klein and Hartmann (1993) have presented a seasonal cycle of low stratiform clouds for ten regions of active stratocumulus convection. Figure 4 displays monthly climatologies of several parameters averaged over the Californian stratus region. Figure 4a demonstrates how closely air temperature tracks the SST, with the air temperature between 0.5° and 1°C cooler than SST. Lilly (1968) explains how this small air-sea temperature difference, and correspondingly weak surface fluxes of sensible heat, cannot be solely responsible for the maintenance of stratus clouds. He argues, rather, that it is strong cloud-top radiative cooling that is responsible for sustaining convection. Figure 4a shows how the 700-mb climatological temperatures have a wider range than surface temperatures. Thus, the annual cycle in static stability (the difference between potential temperature at 700-mb and at the surface) parallels that of 700-mb temperature vice surface temperatures. Stratus cloud amounts peak during June-July-August (the same season as the peak static stability) at around 67% while the minimum stratus occurs in December-January-February at around 45% (Figure 4b). Divergences of surface winds are typically $3 \times 10^{-6} s^{-1}$, with no measurable seasonal cycle (Figure 4c). The seasonal cycle strength of the subtropical high of the North Pacific (strongest in July and weakest in October) parallels that of the stratus cloud amount (Figure 4c).

All shiptrack studies in the Californian stratus region parallel the climatology of stratus development in that tracks occur most frequently in June, July and August, the periods of maximum low-level cloudiness and highest static stabilities. It should be noted, however, that static stability has not proven to be a good predictor of stratus cloudiness on a daily time scale and therefore its use as a predictor of tracks is unreliable.

C. MARINE ATMOSPHERIC BOUNDARY LAYER (MABL)

One of the hypotheses of the MAST experiment is that shiptracks develop in shallow MABLs. The simplest model of the MABL consists of three layers: a shallow

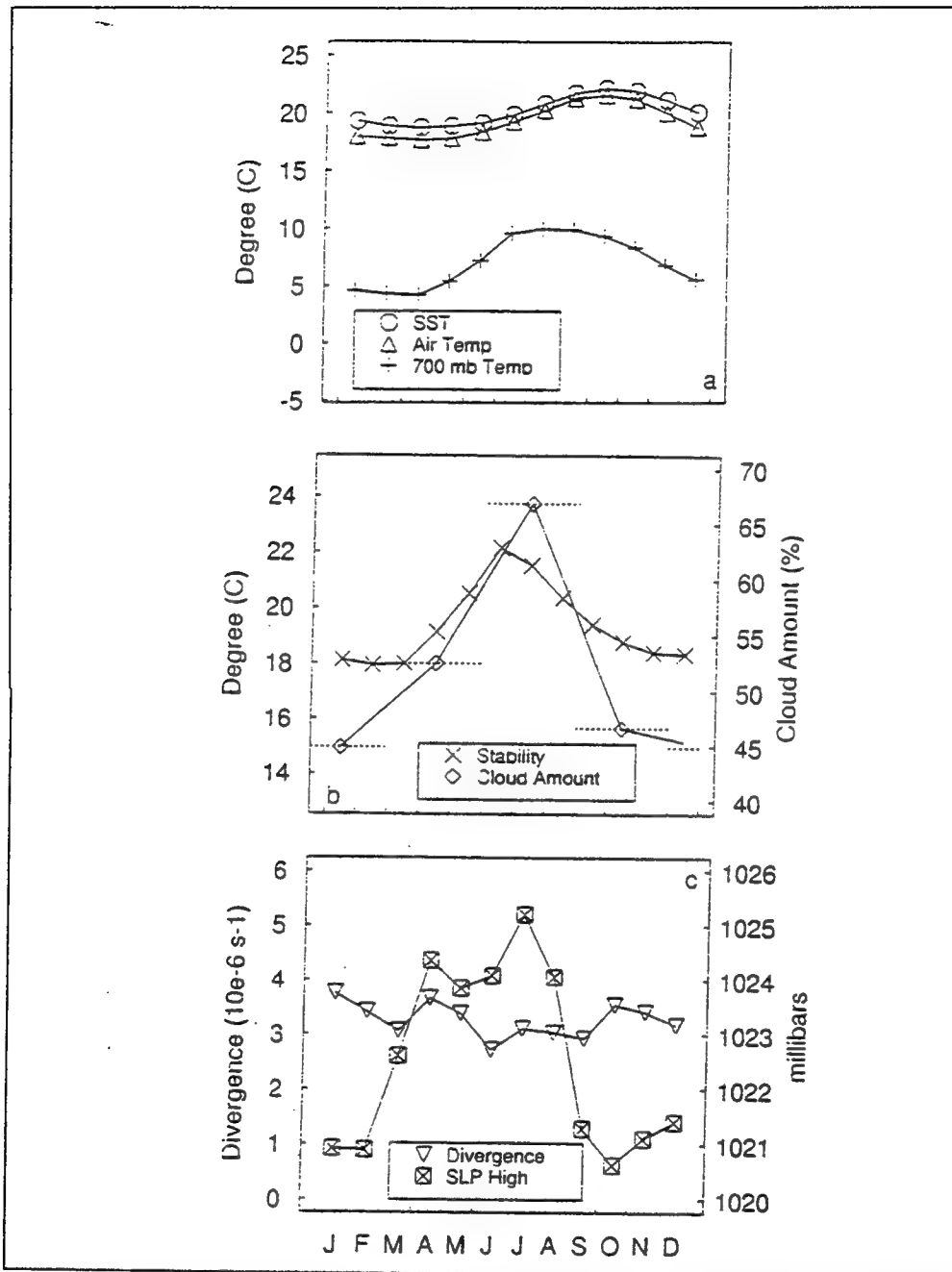10

Figure 4. The annual cycle of cloud, thermodynamic, and dynamic properties for the Californian stratus region: (a) the sea surface, surface air, and 700-mb temperature; (b) the lower-tropospheric stability, and stratus cloud amount (seasonally averaged); and (c) large-scale divergence of surface winds and the peak surface pressure of the subtropical high. (From Klein and Hartmann, 1993).

11

slightly unstable *surface layer*, the *mixed layer* which comprises 35-80% of the boundary layer, and a thin *entrainment zone*, which represents a transition between the boundary layer and the free atmosphere (Stull, 1988). The mixed layer is so named because vertical mixing in the layer leads to conservation of certain properties over its depth. Some variables that are conserved in the mixed layer are mixing ratio, potential temperature, equivalent potential temperature, humidity, and to some extent even wind direction and speed. In an idealized "Jump" model of the mixed layer, these properties are constant with height and then experience a discontinuous jump at the top of the boundary layer. In the case of the California stratus, this jump at the top of the boundary layer marks the base of the strong trade inversion discussed in the previous section. Marine stratus clouds are confined to the boundary layer with cloud top located at the base of the inversion. Figure 5 presents the "Jump" model and demonstrates some of the conserved properties.

Figure 6 is a plot of variables determined from an actual atmospheric sounding from the MAST experiment. Note the conservation of mixing ratio, potential temperature and equivalent potential temperature in the boundary layer as illustrated in the "Jump" model. The abrupt discontinuity in the profiles above 600 meters marks the subsidence inversion.

Figure 7 is a profile of the same sounding plotted on the DOD form WPC 9-16Q (Skew-T, Log P diagram). Note the conservation of equivalent potential temperature in the boundary layer. The profile follows a dry-adiabat to the lifting condensation level (LCL) and a saturation adiabat within the cloud. The subsidence inversion is evident at 945-mb by the rapid increase in temperature and corresponding decrease in dewpoint temperature. Stratiform cloud is confined to this shallow MABL with cloud base located approximately at the LCL and cloud-tops located at the base of the inversion. This profile is representative of the environment in which shiptracks develop.

12
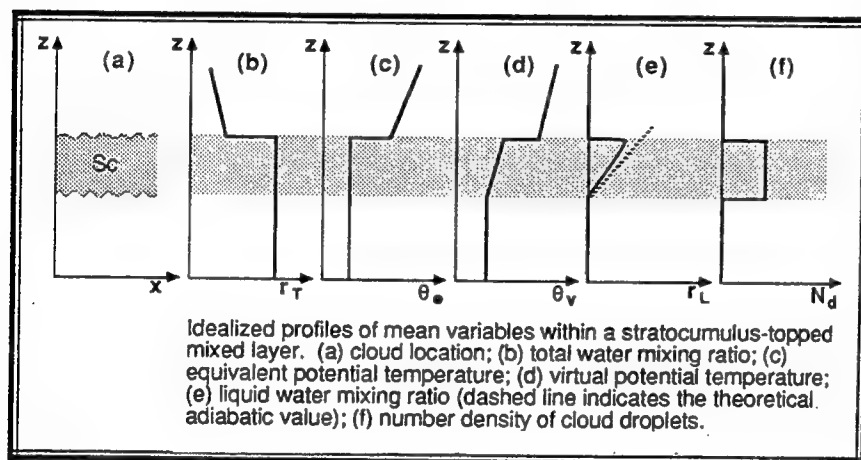
Figure 5. "Jump" Model. Note the discontinuity in variables at inversion base. Stratiform clouds are confined to the boundary layer. (From Stull, 1988).

13
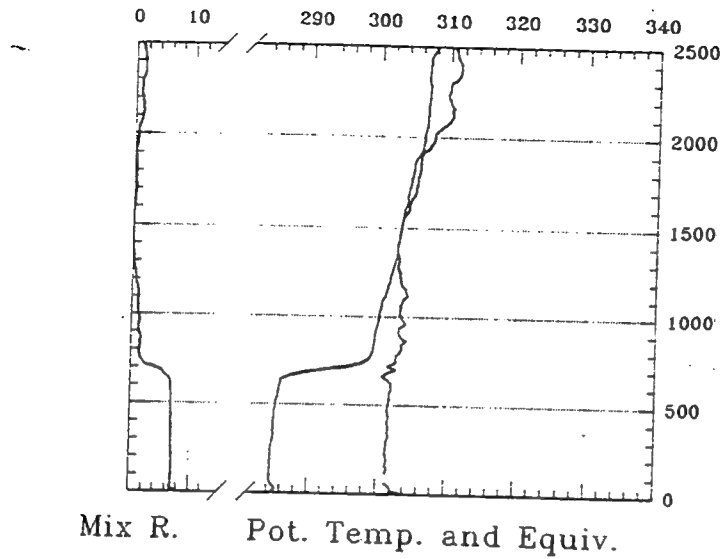
Figure 6. Atmospheric sounding from the MAST experiment depicting conservation of mixing ratio, potential temperature and equivalent potential temperature in a well mixed marine boundary layer. Note the discontinuous jump above 600 m, marking the top of the boundary layer (sounding is from 20 June 1994, 1809 UTC).
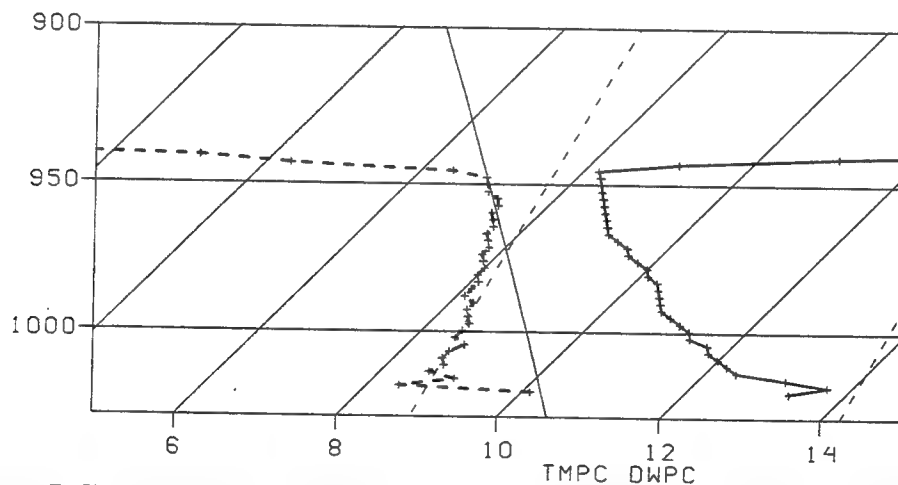
Figure 7. The same atmospheric sounding as depicted in Figure 6, plotted on the Skew-T Log P diagram. The top of the boundary layer is evident near 945-mb. The lifting condensation level (LCL) is marked by a change in slope in the profile from dry-adiabatic (from the surface to 965-mb) to moist-adiabatic (between LCL and the inversion). Stratiform cloud is confined to the MABL between the LCL and the inversion base.

D. SHIP-TRAIL EVOLUTION ABOVE HIGH UPDRAFT NAVAL TARGETS

1. SEAHUNT Organization and Objectives

SEAHUNT was an ocean experiment conducted in July 1991 onboard the Research Vessel (R/V) Egabrag (Porch et al., 1992). The experiment was conducted over a three week period in the waters off the California/Mexico Baja region, with R/V Egabrag returning to port for one day each week for supplies and personnel changes. R/V Egabrag acted as both an upper-air and surface observation platform.

The objective of SEAHUNT was to study the effects of various forcing mechanisms on marine stratiform clouds (Porch et al., in press). A key area of investigation was the forcing associated with shiptracks. SEAHUNT is noteworthy in that it is the first extended field study designed specifically to investigate the environment in which shiptracks develop. The next section discusses only that portion of the data collected during SEAHUNT which was utilized for this thesis.

2. SEAHUNT Data

a. Upper Air

R/V Egabrag conducted an average of two radiosonde launches daily at approximately 12 hour intervals to coincide roughly with 1200 and 2400 UTC. These atmospheric soundings were sampled every five seconds, approximately every 10-15 meters, up to 300 observations. From this data, boundary layer heights were determined. These soundings will be used in conjunction with the satellite data discussed below.

b. Meteorological Station Data

Personnel aboard R/V Egabrag recorded SSTs in conjunction with the radiosonde launches described above as well as comments on sky conditions at the time of launch. There are several gaps in this data in that there is no record of SST and/or comments associated with some of the soundings. The impact of this is considered minor.

c. Satellite (AVHRR) Data

Data tapes of HRPT telemetry data (NOAA 11 only) were acquired for the month of July 1991 and converted to AVHRR datasets. These datasets consist of:

- AVHRR Channel 1, 0.58 - 0.68 μm, red-visible,

- AVHRR Channel 2, 0.72 - 1.10 μm, red-visible/near infrared,

- AVHRR Channel 3, 3.55 - 3.93 μm, near infrared,

- AVHRR Channel 4, 10.3 - 11.3 μm, thermal infrared,

- AVHRR Channel 5, 11.5 - 12.5 μm, thermal infrared

AVHRR sensor counts were radiometrically calibrated. For channels 1 and 2, the units are percent albedo; for channels 3 through 5, the units are brightness temperature. A subset of these datasets, containing the region of study during SEAHUNT, was extracted from each dataset.

E. MONTEREY AREA SHIPTRACK EXPERIMENT

1. MAST Organization and Objectives

MAST was a multi-agency effort conducted in June, 1994 as the field program component of the Surface Ship Cloud Effect (SSCE) Accelerated Research Initiative (ARI) sponsored by the Office of Naval Research (ONR). The experiment was conducted in the oceans west of central California. Figure 8 depicts the MAST operating area. The SEAHUNT operating area is also indicated. Several highly traveled shipping lanes transect the operating area. Numerous research platforms were dedicated to this undertaking, including five U.S. Navy ships, the R/V Glorita, three instrumented aircraft and an airship. MAST is the most extensive field study of shiptracks and their environment to date. Specific platforms involved are described in detail in the MAST Operations Plan (ONR, 1994). Per this plan, the primary objective of MAST is to:

16
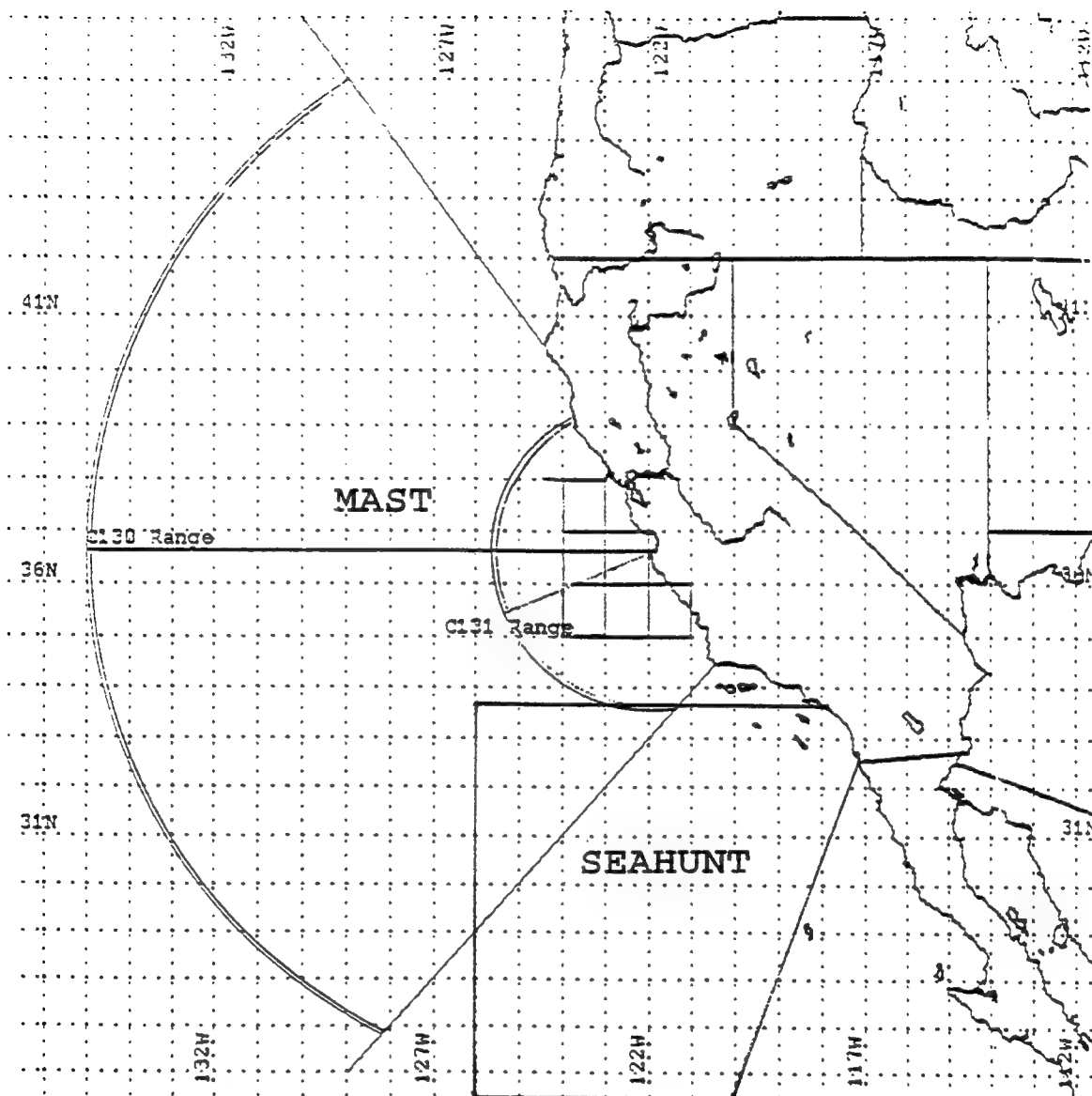
Figure 8. Operating areas for the SEAHUNT and MAST field experiments. The primary region for R/V Glorita is indicated by the grid between the Monterey coast and 124.00°W. Operating ranges of MAST aircraft are indicated by circular arcs.

17

- Determine the ship-related necessary conditions for the formation of surface ship cloud effects in a region and at a time known to support formation of these effects.

Secondary objectives are to:

- Corroborate the ability of the surface ship cloud effects model being developed by the SSCE Project to describe the ship-induced perturbations to the marine atmospheric boundary layer

- Acquire a full set of initial conditions to be used as input to the SSCE model.

These objectives are to be met through the testing of a number of hypotheses addressing

- Aerosol/Cloud Interactions and Detailed Microphysics

- Boundary Layer Perturbations by Ships

- Cloud Dynamics

- Background Environmental Conditions

Hypotheses pertinent to this thesis are:

(1) Shiptrack formation requires a set of background conditions which involve low boundary layer depth, CCN concentration below a given threshold, and pre-existing cloud formation mechanisms.

(2) A decoupled marine boundary layer inhibits transport of ship effluent to upper cloud.

Data collected for the MAST experiment is much more extensive than for SEAHUNT. That portion of the data collected during MAST used in the preparation of this thesis is discussed in the next section.

2. MAST Data

a. Upper Air

The R/V Glorita conducted an average of six radiosonde launches daily at roughly four hour intervals. These atmospheric soundings were interpolated at 20 meter intervals up to 1000 observations. Measured parameters were pressure, temperature and relative humidity. Derived quantities include height, dewpoint and mixing ratio. The formulae and procedures used to calculate mixing ratio, dewpoint and height are included as Appendix II to this document. Boundary layer heights were determined from this data. These soundings will be used in conjunction with the satellite data below.

b. Meteorological Station Data

Hourly measurements of SST, air temperature, relative humidity, and wind direction and speed were recorded by R/V Glorita personnel. Comments on sky conditions at launch time as well as two hours prior were also recorded. There are some gaps in the SST data due to periods when the temperature sensor was not in the water. This is considered minor and will be expanded on in Chapter III.

c. Satellite (AVHRR) Data

HRPT telemetry data was collected at the Naval Postgraduate School. Datasets of NOAA-9,10,11, and 12 AVHRR data were created and archived. These datasets consist of the same data elements (AVHRR Channels 1-5) as the SEAHUNT set.

19

III. METHODOLOGY

A. SEAHUNT

A total of 33 radiosonde profiles (designated EB01-EB33) and accompanying logs from the R/V Egabrag were analyzed. The sounding data was plotted on Skew-T Log P diagrams and comments from the logs noted.

The NOAA-11 AVHRR datasets were then examined to identify those satellite images closest in time to the soundings. Given the relatively stagnant environmental conditions required for the development of long ship tracks, a maximum time difference of three hours between sounding and satellite image was chosen as criteria to identify sounding/image pairs. Subsets (512x512 km) of the AVHRR data centered on the research vessel position were extracted from the data tapes and processed using the TeraScan software package developed by SeaSpace Corporation. The satellite images were mapped to a mercator projection and navigated. The location of R/V Egabrag at the time of the accompanying sounding was noted and the AVHRR Channel 3 image was examined for ship tracks in the vicinity of R/V Egabrag. The goal here is to determine if the sounding was taken in a *track-conducive* environment. The AVRRR Channel 4 (11 µm, thermal infrared) radiance value of a 7x7 km box centered on the position of the research vessel was determined. Temperatures within ± 0.5°C of this value were highlighted in the image. In a dry-adiabatic atmosphere, there is an average temperature change of 10°C/km, thus a maximum temperature gradient of 0.5°C equates to a maximum height difference of 50 meters.

If the cloud-tops are relatively smooth and hence, equal in height, as stratiform clouds generally are, the highlighted region, as described above, should be quite broad. If shiptracks in the Channel 3 image are within the highlighted region, the environment is considered track-conducive and all tracks within the conducive region are counted. Exceptions include those times when highlighted regions were influenced by reduced emmitance from obscuring cirrus clouds or by increased values due to the sensing of surface emission through broken clouds. In these instances, a mean low level cloud-top

21

temperature was determined from neighboring unobscured stratiform fields (within the 300 km constraint) and this value was used in order to determine the region to be highlighted. Again, the concept here is to determine if the research vessel is in a relatively large, uniform cloud regime.

A constant distribution of shipping is assumed throughout the analysis. Observations of shiptracks indicate that when they do develop and persist, they do so in clusters. Shiptrack data extraction performed during MAST revealed that it is extremely rare for only one shiptrack to be present in a cloud-topped region. When environmental conditions are not conducive to track development, there is a noticeable lack of shiptracks over very large regions. Thus, if cloud was present in the image but no shiptracks were detected, the lack of tracks is attributed to environmental factors and not a lack of shipping in the region. The satellite fields are quite large and the likelihood of ship traffic in the field is good. Figure 9 illustrates the validity of this assumption. Positions of all weather reporting ships to the Fleet Numerical Meteorological and Oceanographic Center (FNMOC) for the period 1200-1800 UTC, 17Jun94, are noted. The position of R/V Glorita is indicated also. This figure is typical of the shipping density in the operating area. Of note, the vessel 3FMV3 is the Bosphorus Bridge, a diesel engine ship which was investigated on this day by MAST aircraft. The aircraft profile showed a shallow surface layer and it is believed the plume was trapped within this layer.

If it was deemed that the sounding was indeed taken in a track-conducive environment, the boundary layer (BL) height was determined and recorded. BL height was determined by noting the height of the last decreasing temperature in the temperature profile on the Skew-T before the sharp rise in temperature marking the subsidence inversion. An error of 10% of the BL depth is assumed in allowing the sounding-determined height to be representative of the height over a large region.

Other parameters were also noted and recorded. The lifting condensation level (LCL) was chosen as that point where the temperature profile deviated from a dry-adiabat to a saturation adiabat. Cloud thickness was determined by subtracting the LCL from the
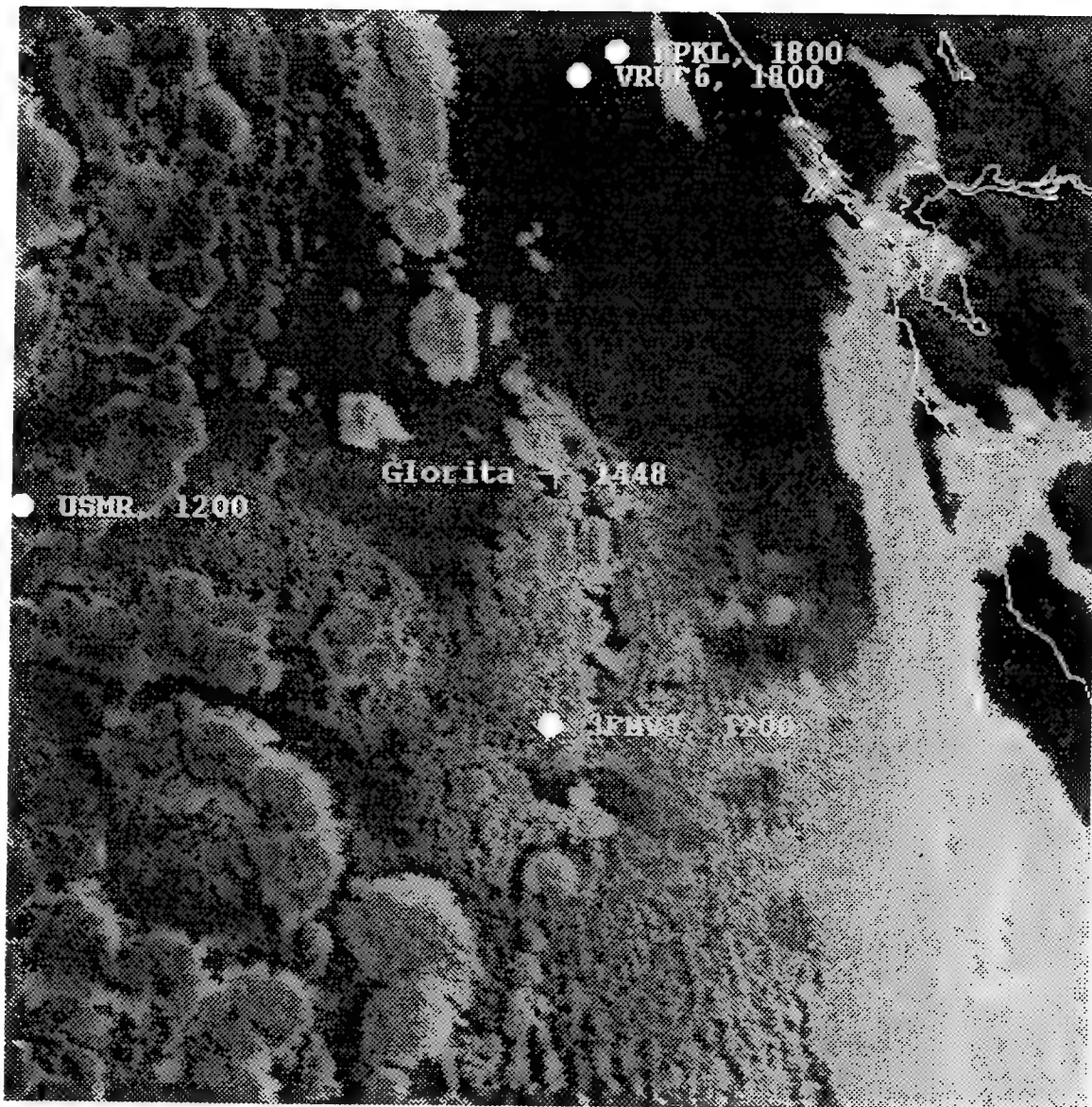
22

Figure 9. Positions of weather reporting ships to Fleet Numerical Meteorology and Oceanography Center for the period 1200-1800 UTC, 17 June 1994.

BL height. Also, a 2°C dewpoint depression was used as additional criteria in determining if cloud was present.

Figures 10-12 illustrate this process. Figure 10 is sounding EB06 and Figure 11 is its accompanying AVHRR channel 3 image. The time difference between sounding and image is 55 minutes. The spatial difference between R/V Egabrag and the closest shiptrack is 22 km.

Figure 12 is the corresponding AVHRR Channel 4 image for this same satellite pass. The satellite retrieved mean cloud-top temperature for the 49 km^2 box centered on the R/V Egabrag's position is 11.24°C. The region of 10.74-11.74°C has been highlighted (white), revealing that much of the region meets the imposed temperature criteria.

There are several shiptracks within this temperature field. Having met the spatial and temperature criteria set forth (within 300 km and ± 0.5°C), and it is determined that the sounding is representative of a track-conducive environment. Tracks within the required parameters are counted and pertinent information from the sounding and measured surface parameters is recorded for analysis.

Sounding/image pairs that did not meet the three hour temporal constraint were dismissed from this study as were those pairs where insufficient cloud cover precluded development of a track (e.g., clear air or broken-cloud conditions). A total of eight soundings were dismissed from the SEAHUNT data set.

B. MAST

A total of 94 radiosonde profiles (designated GL01-GL94) and accompanying surface data from R/V Glorita were obtained and plotted.

Datasets from NOAA-9,10,11 and 12 were processed and sounding/image pairs were identified and studied. In general, the same criteria for selection used in the SEAHUNT dataset was adhered to with a few exceptions. Sounding/image pairs with a time difference greater than three hours were still retained if the case immediately before and the case immediately after were both track-conducive and shiptracks from the case

24
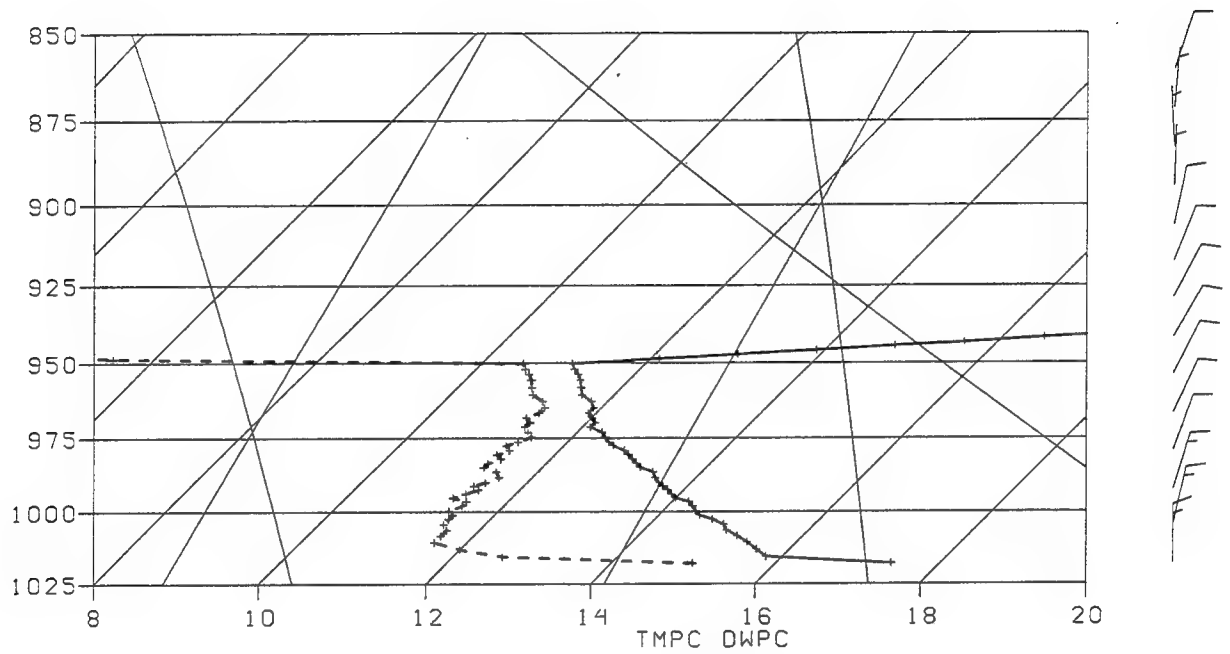
Figure 10. Sounding EB06, 12 July 1991, 1200 UTC.
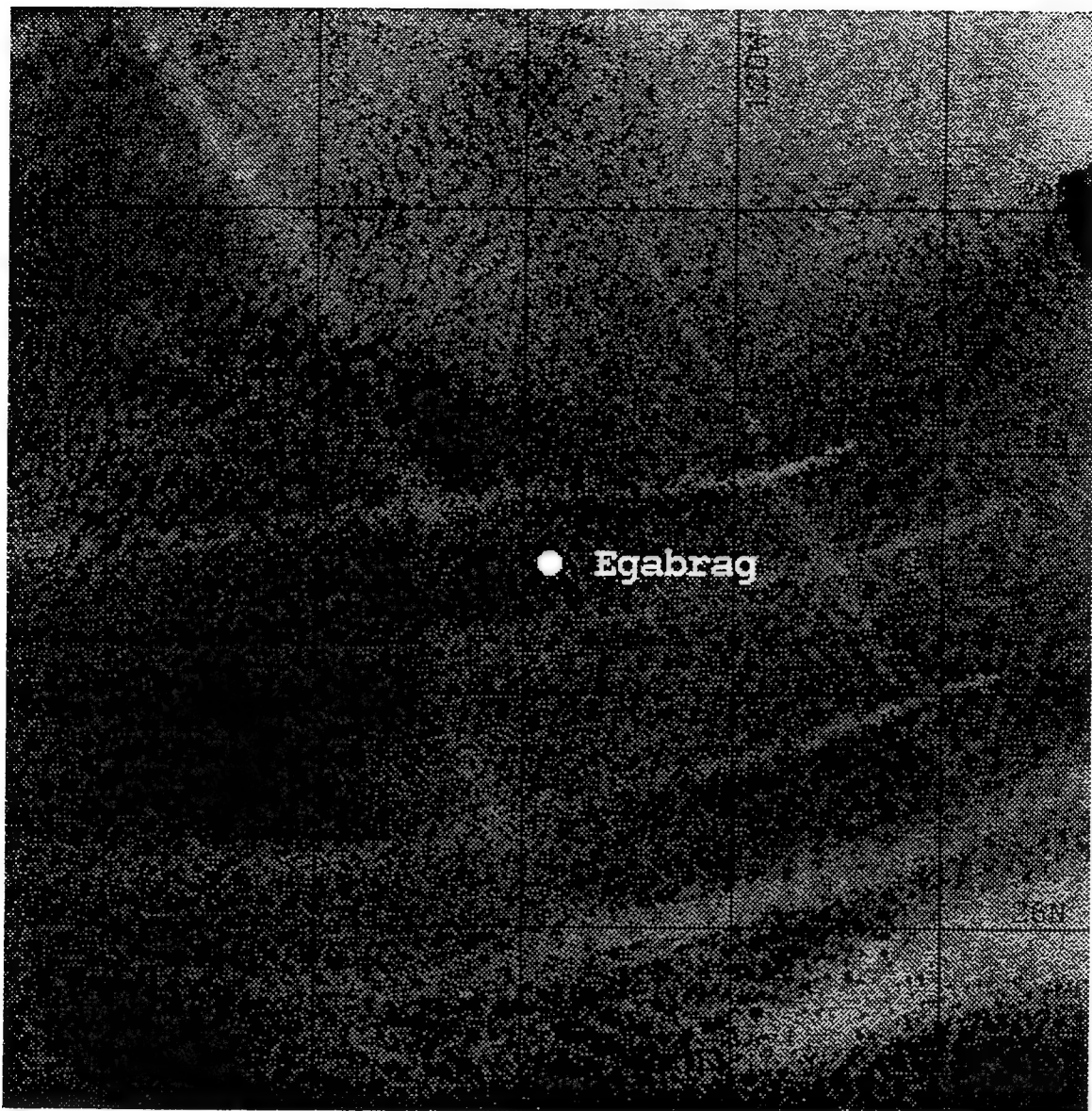
Figure 11. NOAA 11, AVHRR Channel 3 image from 12 July 1991, 1101 UTC. Location of R/V Egabrag is indicated. Distance between R/V Egabrag and the shiptrack to the south is approximately 20 km.

Figure 12. NOAA 11, AVHRR Channel 4 image from 12 July 1991, 1101 UTC depicting a large homogeneous cloud-topped marine region. Cloud-top temperature in the vicinity of R/V Egabrag is 11.24°C. The region of 10.74-11.74°C has been highlighted white.

prior were still evident in the case after. A total of 54 sounding/image pairs were dismissed from the MAST dataset due to inadequate temporal resolution or insufficient cloud.

IV. ANALYSIS/RESULTS

A. SEAHUNT

1. Conducive Environments

Table 2 lists all R/V Egabrag soundings, accompanying AVHRR image and a general comment regarding its analysis. As previously noted, eight sounding/image pairs were dismissed, leaving a total of 25 sounding/image pairs available for this period. Figure 13 is a plot of boundary layer depth for these 25 cloud-topped MABLs. R/V Egabrag was in a track-conducive environment in 14 cases. Two of these cases will be presented, followed by two cases in which a cloud-topped MABL was present but there were *no* shiptracks present.

a. EB06

Sounding EB06 was launched at 1101 UTC on 12Jul91 at 27.55°N-120.88°W. The corresponding image is n11.91193.1101 (Figure 14). R/V Egabrag is well located in a track-rich environment with a BL height of 580 m. The sounding (Figure 15) shows the environment to be superadiabatic in the surface layer, above which the profile is dry-adiabatic. A superadiabatic surface layer exists in nearly all of the R/V Egabrag soundings. It is believed that the influence of deck heating on the research vessel led to high initial temperatures recorded in these profiles and thus the appearance of a superadiabatic surface layer. As such, the possibility of a relationship between a superadiabatic surface layer and shiptrack development is not considered. It should be noted that the MAST dataset has no such trend in the data, providing additional support for this conclusion. The deviation in the profile from dry-adiabatic to moist-adiabatic at 971-mb (390 m) marks the LCL and cloud base. The profile is moist-adiabatic through the cloud and dewpoint depression is less than 1°C. The boundary layer is capped by the strong, very dry subsidence inversion at 950.2-mb (580 m). Cloud thickness is 190 m, making up 32.7% of the BL depth.

29
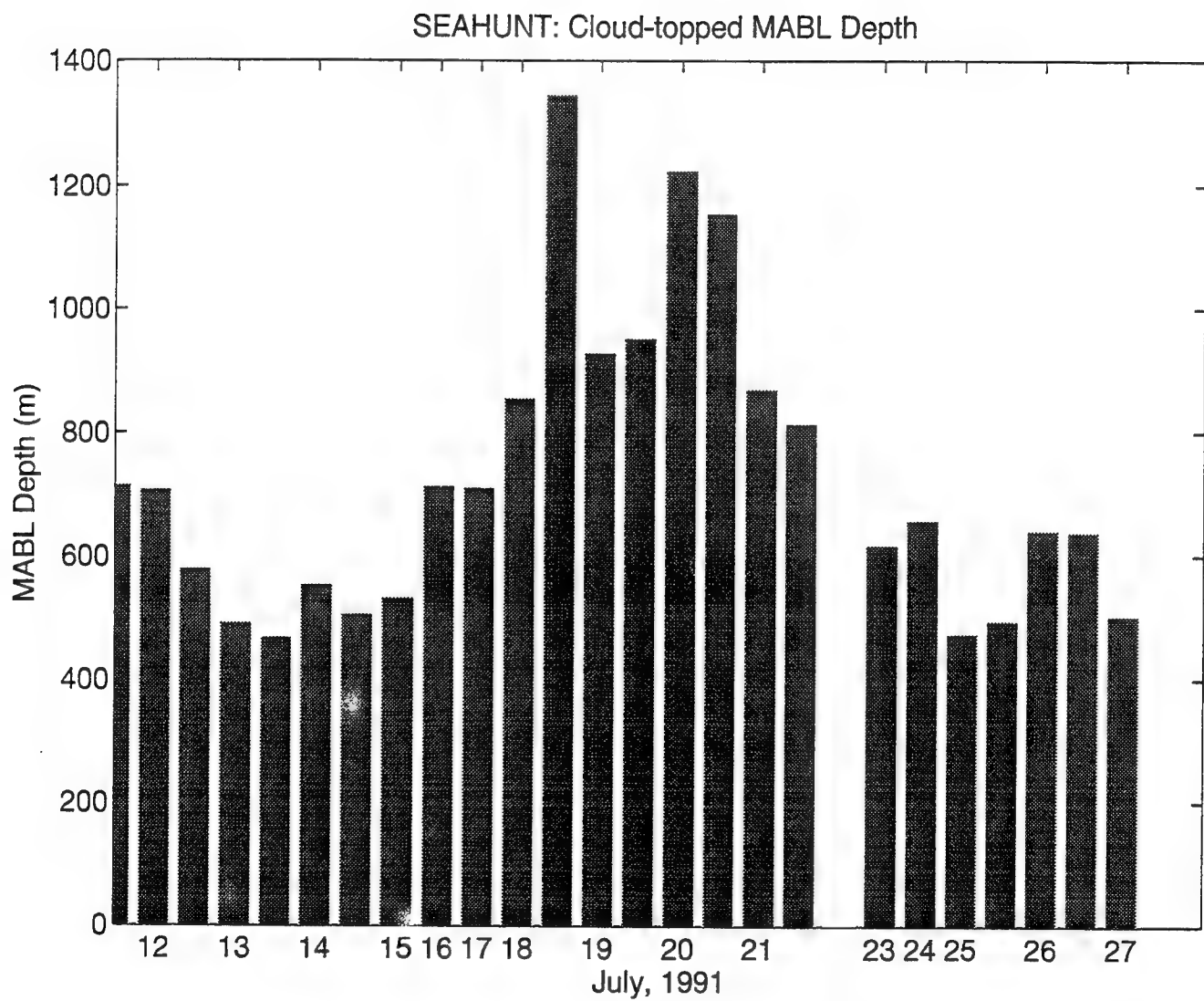
Figure 13. MABL depth for the 25 cloud-topped cases from SEAHUNT.
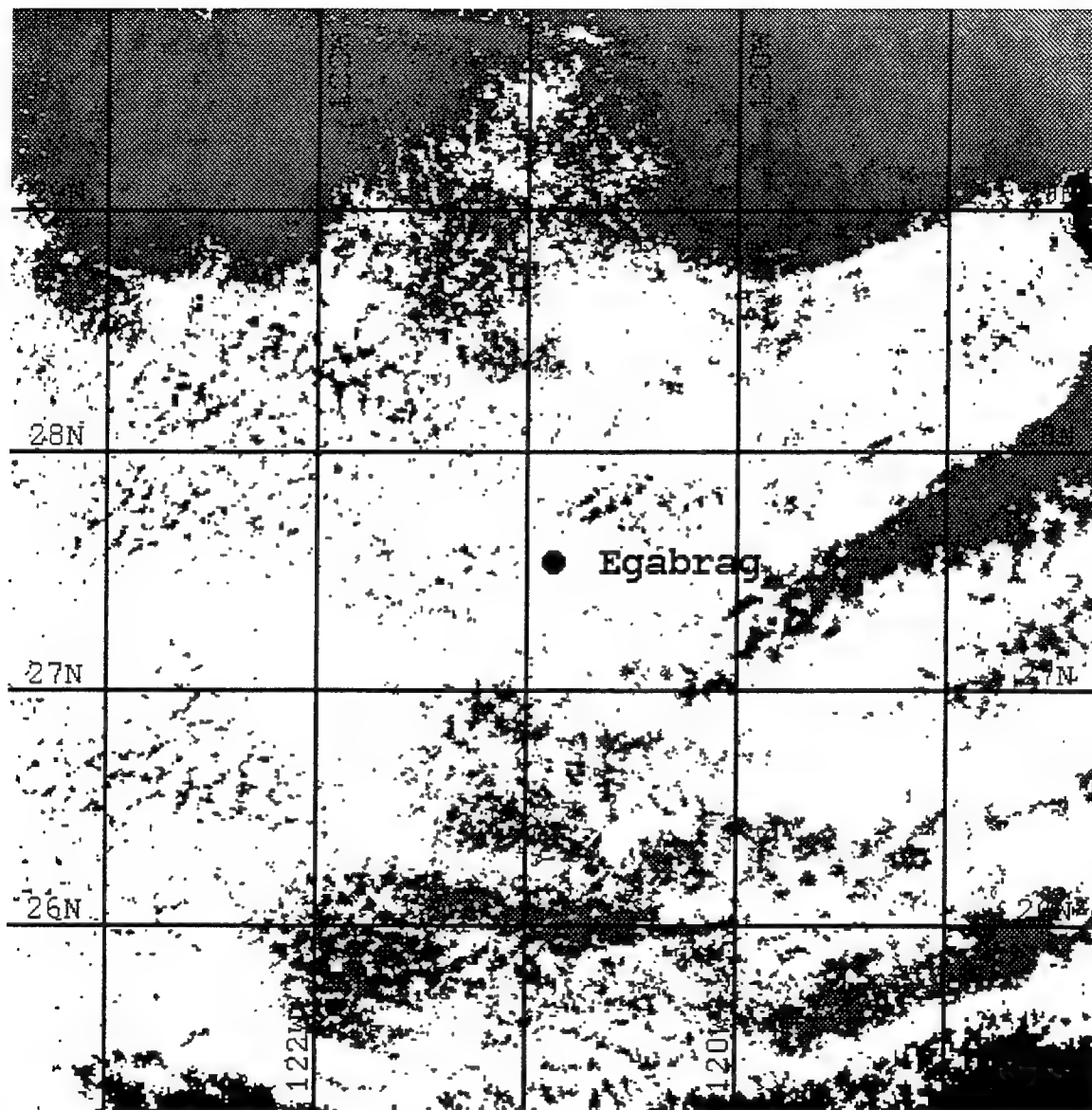
Figure 14. NOAA 11, AVHRR Channel 3 image from 12 July 1991, 1101 UTC. Location of R/V Egabrag is indicated.
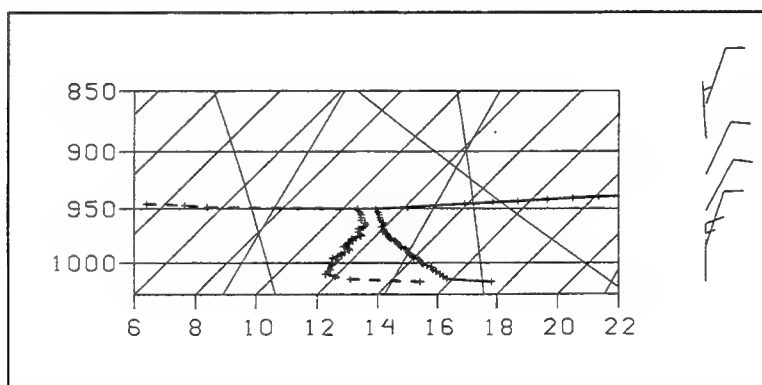
Figure 15. Sounding EB06, 12 July 1991, 1200 UTC.

31

SST (18.2°C) is warmer than the overlying air temperature (17.2°C) and winds are from the N/NE at 7.7 m/s at the surface, decreasing in strength to 6 m/s at the top of the BL. Surface pressure is 1017.9-mb and relative humidity is 86%.

b. EB28

Sounding EB28 was launched at 1200 UTC on 25Jul91 at 33.48°N-121.93°W. R/V Egabrag is again well positioned with respect to tracks in the corresponding satellite image, n11.91206.1151 (Figure 16). BL depth is 496 m. Figure 17 reveals the environment to be dry-adiabatic to the LCL at 987.3-mb (233 m) and moist through a cloud of thickness 263 m to the inversion base. Cloud makes up 53.0% of the boundary layer depth.

SST was not recorded for this sounding. Air temperature is 15.4°C. Winds are from the NW at an average of 7.5-10 m/s in the boundary layer. This case is noteworthy in that the winds are about twice the magnitude of the winds in the other track-conducive cases. Surface pressure is 1015.0-mb and relative humidity is 94%.

c. Track-conducive Synopsis

Of the 14 conducive cases, boundary layer depth is between 496 and 711 meters. Clouds vary greatly in thickness with drizzle encountered on two occasions. SST is greater than the overlying air temperature in four cases and there are six cases where the air temperature is greater than SST. SST was equal to air temperature in only one case and SST was not recorded in three instances. In all but two cases, the air-sea temperature difference is less than 1°C. Winds are from a generally northerly direction and vary from 2.1-11.3 m/s at the surface attaining a maximum of 38 m/s within the boundary layer in one instance. Surface pressures are between 1014.3-mb and 1019.3-mb. Relative humidities are between 72% and 99%. Table 3 displays information available relative to all track conducive cases from SEAHUNT. Note that boundary layer depth is less than 750 m in all cases.
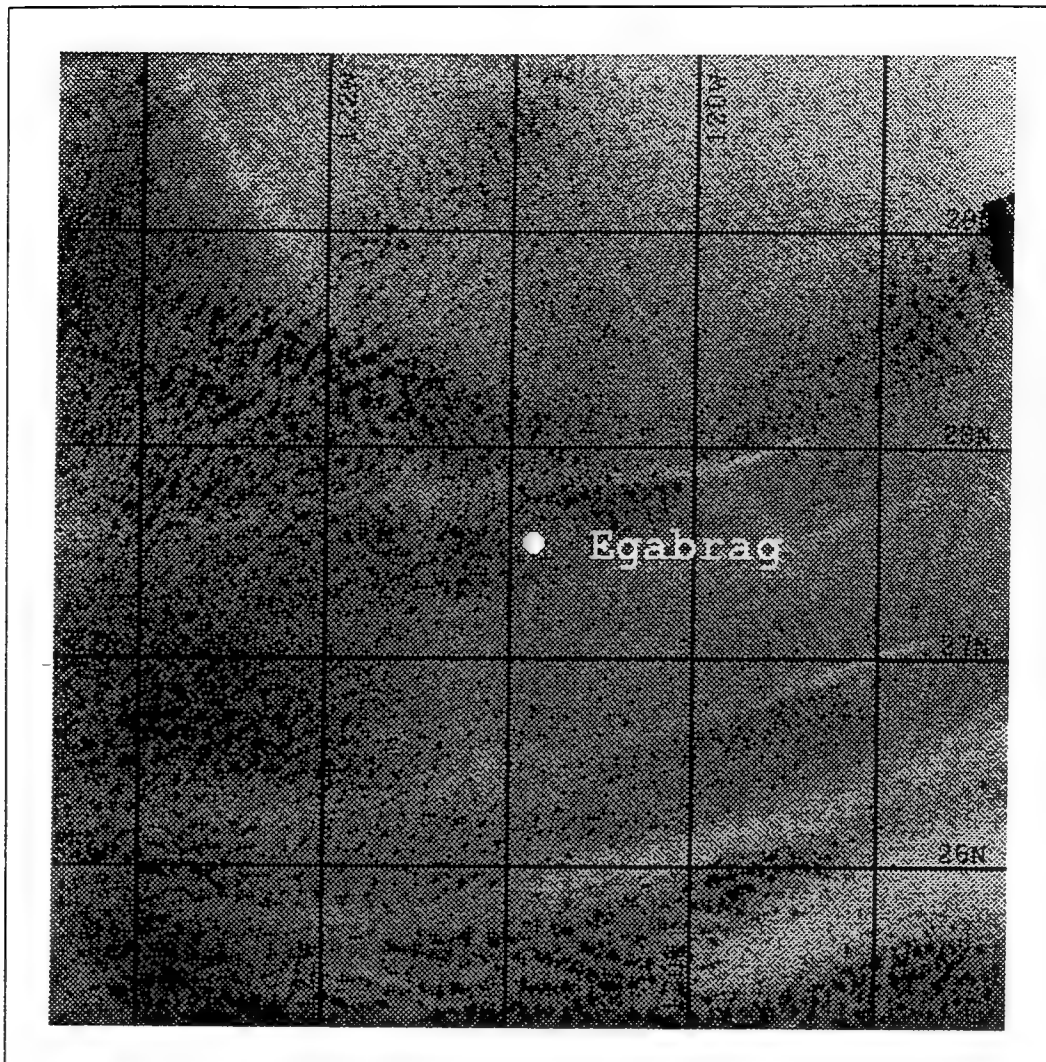
Figure 16. NOAA 11, AVHRR Channel 3 image from 25 July 1991, 1151 UTC. Location of R/V Egabrag is indicated.

Figure 17. Sounding EB28, 25 July 1991, 1200 UTC.

2. Non-Track Cases

There were 11 instances from the SEAHUNT period where sounding/image pairs revealed that stratiform cloud was present in the boundary layer but there were no shiptracks. Table 4 lists pertinent information for these non-track cases. Nine of these soundings (EB16-EB24) were continuous and extend over the period of 18-23 July 91. Over this period, there is a substantial rise in marine boundary layer depth due to changes in synoptic conditions. A large scale disturbance south of the operating area modified the large scale flow, leading to increased mixing and an increased boundary layer depth in the operating area. There were no shiptracks observed in the clouds off the coast of southern California during this period. Two of these non-track cases will be presented as well as additional comments that may shed light on the nature of shiptracks.

a. EB21

Sounding EB21 was launched at 1200 UTC on 20Jul91 at 32.34°N-120.97°W. The corresponding image is n11.91201.1107 (Figure 18). Figure 19 shows the environment to be unstable with respect to dry processes to 952.8-mb (536 m) and moist-adiabatic to 884.4-mb (1155 m). Cloud thickness is 619 m, making up 53.6% of the boundary layer. R/V Egabrag logs indicate that drizzle is detected. Ackerman et al. (1993) have hypothesized that drizzle may play an important role in shiptrack development. As drizzle depletes clouds of CCN, the environment may become more susceptible to shiptrack production as the ratio of ship-produced CCN to background CCN increases.

SST (15.9°C) is slightly warmer than the overlying air temperature (15.8°C). Winds veer from WNW to NW and decrease in speed from 10.5 m/s in the lower boundary layer to 7.2 m/s at the top of the MABL. Surface pressure is 1015.5-mb and relative humidity is 95%.

Note that all parameters except BL depth (1155 m) are within the threshold of the track-conducive environment of Table 1. It would appear that while drizzle may lower background CCN concentrations and perhaps aid in the development of shiptracks, boundary layer depth plays a key role in how effective that mechanism is.

Figure 18. NOAA 11, AVHRR Channel 3 image from 20 July 1991, 1107 UTC. Location of R/V Egabrag is indicated.
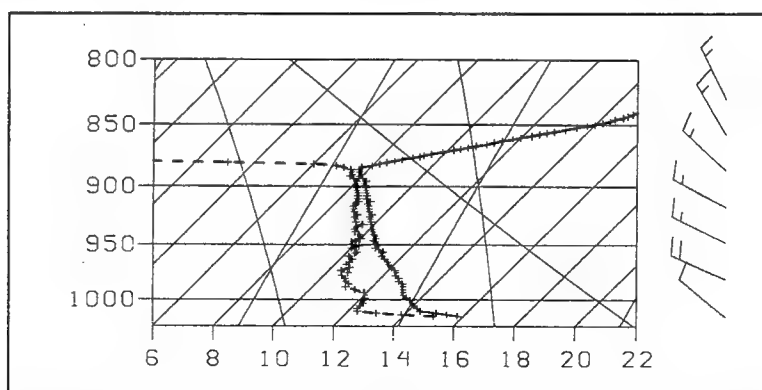
Figure 19. Sounding EB21, 20 July 1991, 1200 UTC.

b. EB22

Sounding EB22 was launched at 0000 UTC on 21Jul91 at 32.90°N-120.33°W. The corresponding image is n11.91201.2229 (Figure 20). Boundary layer depth is 871 m and there are no shiptracks present. Figure 21 indicates a superadiabatic layer from the surface to 973.7-mb (307 m). It is highly unlikely that the environment could support such a deep superadiabatic layer and the data is suspect in this part of the sounding. Of significance in this example is the stable layer between 971.8-mb (385 m) and 968.5-mb (413 m). The LCL is located at 941.4-mb (650 m) and the profile is moist to the inversion at 916.7-mb (871 m). Cloud thickness is 221 m, making up 25.4% of the boundary layer.

SST (16.8°C) is cooler than the overlying air temperature (18.1°C). Winds veer from NW to N and vary from 2-6 m/s in the boundary layer. Surface pressure is 1017.0-mb and relative humidity is 72%.

This case is important because it supports the MAST theory that a decoupled boundary layer inhibits shiptrack production.

c. Additional Comments

The following comments address cases not featured individually in the text of this thesis. They aid in understanding the complex nature of shiptracks.

- BL height is 533 m and SST is greater than the overlying air temperature. R/V Egabrag is located just offshore in the vicinity of a small scale circulation. Additionally, the clouds are exceptionally bright in the imagery and appear to be contaminated by continental sources of aerosol. The combination of more vigorous circulation and masking by the aerosol may explain the lack of ship tracks in the shallow boundary layer clouds of this case.

- EB24 is the last sounding of the long period of increased BL depth prior to track detection in EB25. Table 4 reveals the BL depth to be decreasing over the period 19-23 Jul.

- BL depth is greater for EB25 (shiptracks) than in sounding EB24 (no shiptracks). R/V Egabrag logs indicate that light drizzle was detected for EB25. This provides additional evidence that drizzle may play an important part in cloud-cleansing and in shiptrack production.
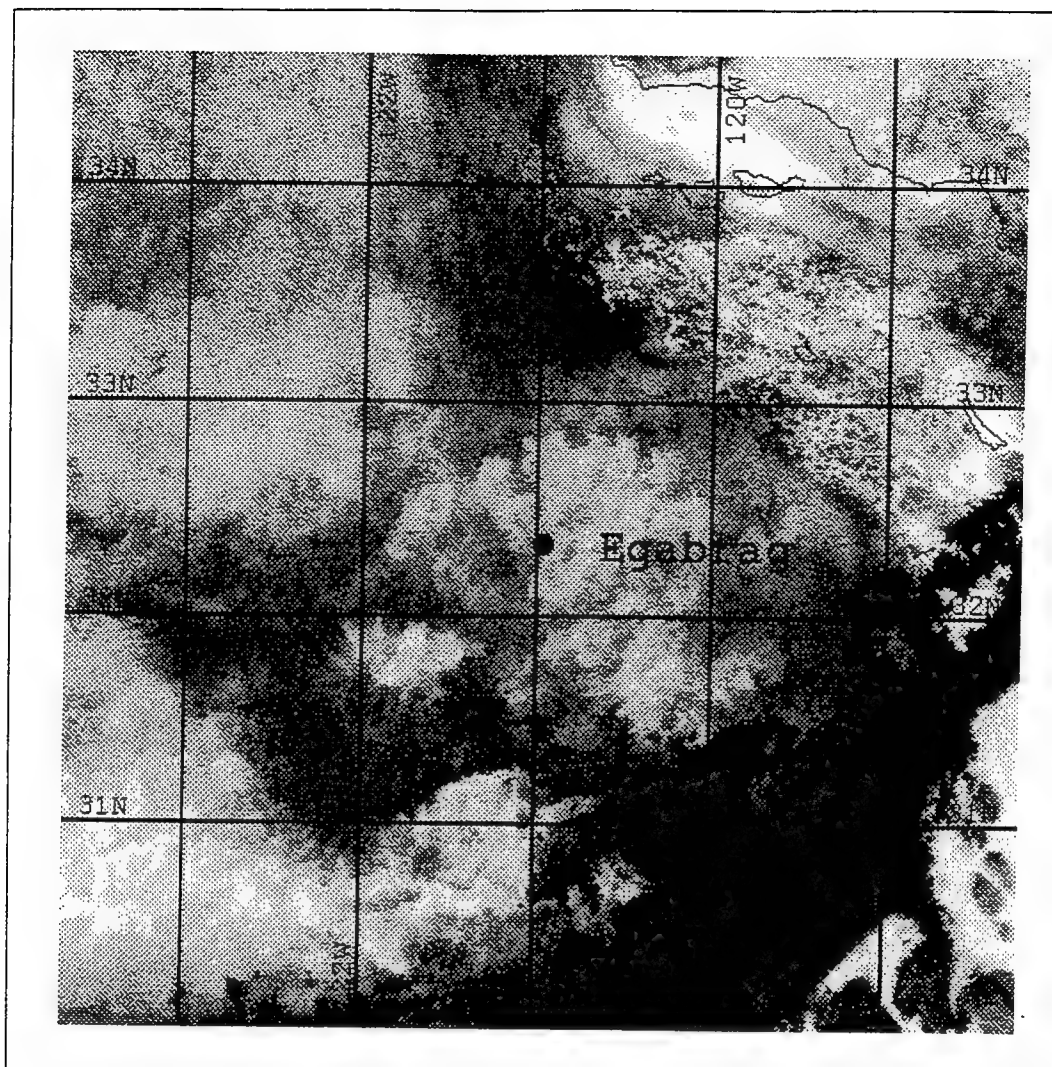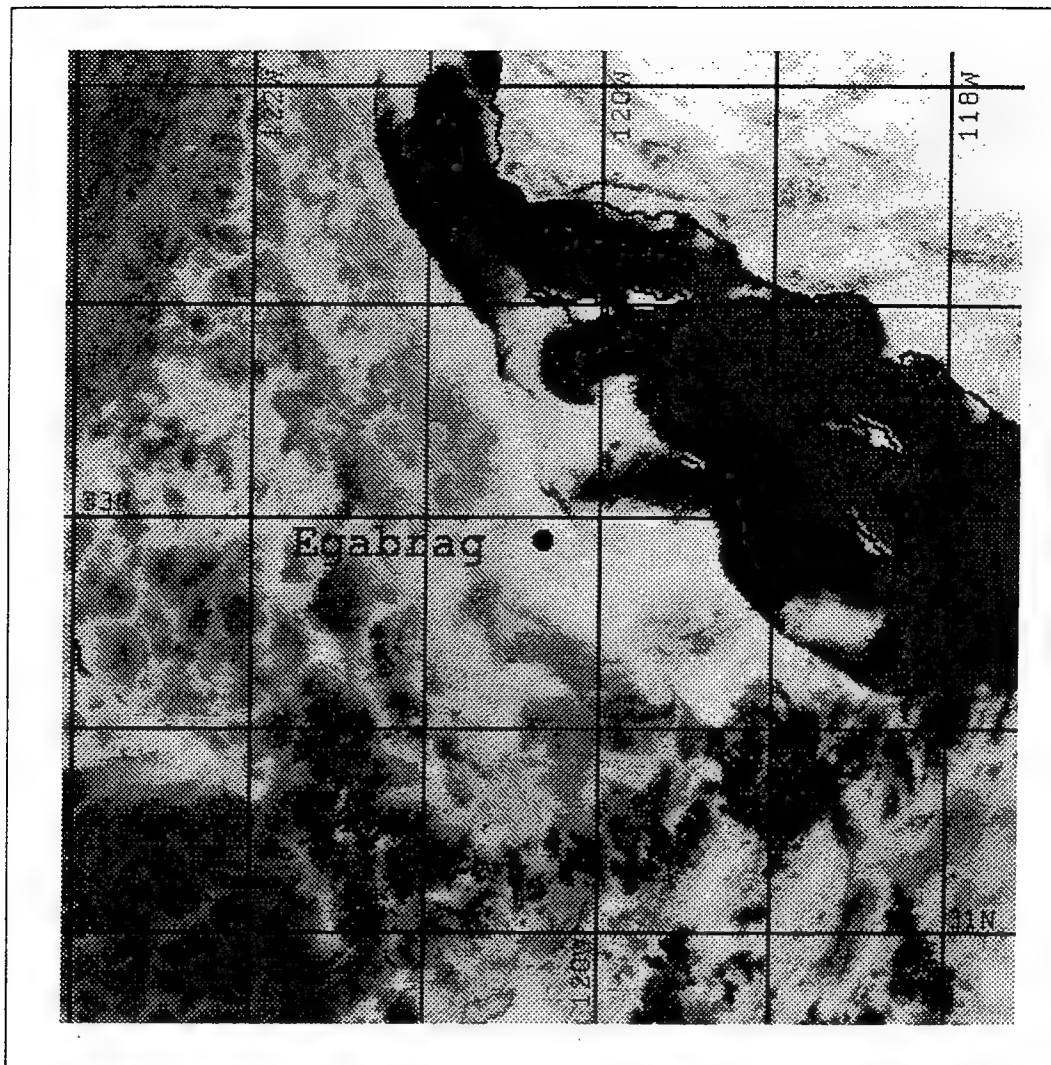
Figure 20. NOAA 11, AVHRR Channel 3 image from 20 July 1991, 2229 UTC. Location of R/V Egabrag is indicated.
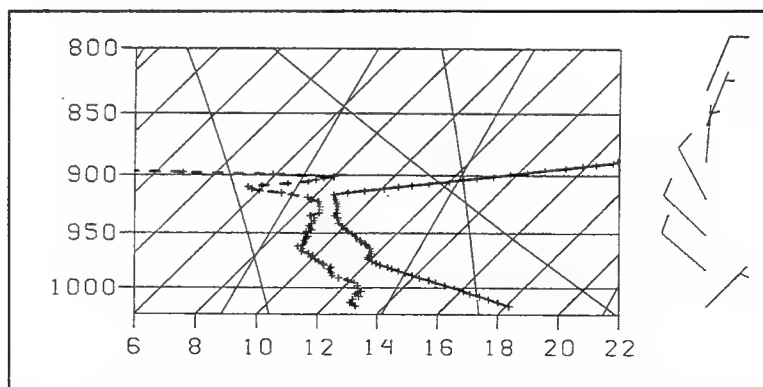
Figure 21. Sounding EB22, 21 July 1991, 0000 UTC.

3. SEAHUNT Summary

Although the SEAHUNT dataset is a small one, there is something to be taken away from it before examining the MAST dataset. Ship tracks appear to be closely tied to boundary layer depth. Figure 22 is a histogram of the 25 cloud-topped marine boundary layers from SEAHUNT. Shading indicates the occurrence of shiptracks. Note that in this distribution of boundary layer height with stratiform cloud present, shiptracks occur on the lower end of this distribution. This is strong evidence that track development is closely tied to boundary layer depth. Individual case studies presented support this conclusion as well. Of the 14 track-conducive cases, only two occur in MABL depths exceeding 700 m.

No tracks were present in the one decoupled boundary layer sampled during this period, supporting the hypothesis that an internal stable layer would tend to inhibit the upward transport of aerosol to cloud base, preventing track formation. Additionally, while the role of drizzle may be important to the development of shiptracks, boundary layer depth plays a key role in how effective that mechanism is.

This analysis also reveals that the occurrence of SSTs greater than the overlying air temperature may also be important to track formation processes. It is believed, however, as the climatology would suggest, that this is a characteristic relevant to the formation of the stratiform cloud itself and not directly linked to the formation of ship tracks except as a cloud production mechanism.

B. MAST

1. Conducive Environments

Table 5 lists all R/V Glorita soundings, accompanying AVHRR image and a general comment regarding its analysis. A total of 40 sounding/image pairs were deemed usable for this period. Figure 23 is a plot of boundary layer depth for each of the soundings. R/V Glorita was in a track-conducive environment in 35 cases. Two of these cases will be presented, followed by two cases in which a cloud-topped MABL was present but there were no shiptracks observed.

38
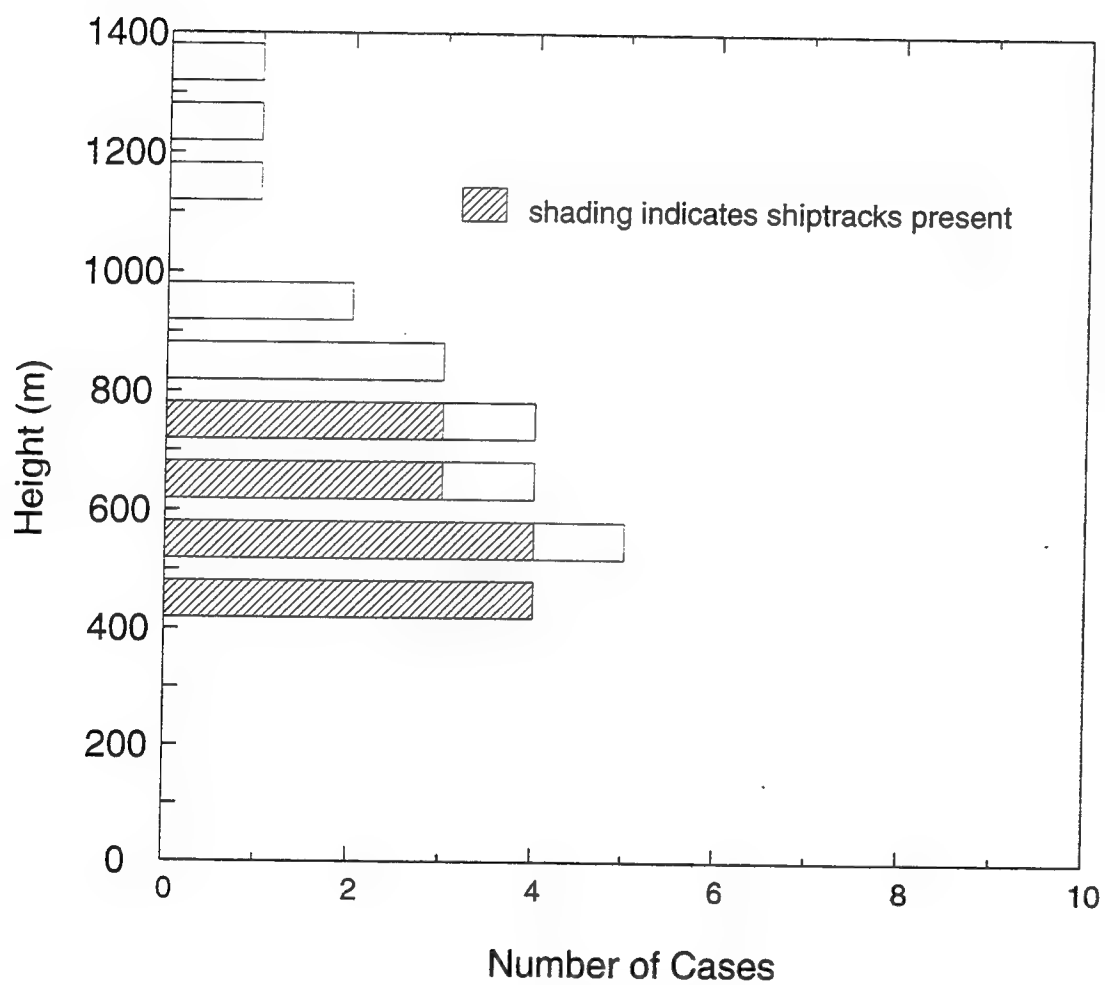
Figure 22. Histogram of all cloud-topped MABLs from SEAHUNT. Shading indicates the presence of shiptracks. Shiptracks were present in boundary layers up to 750 m.
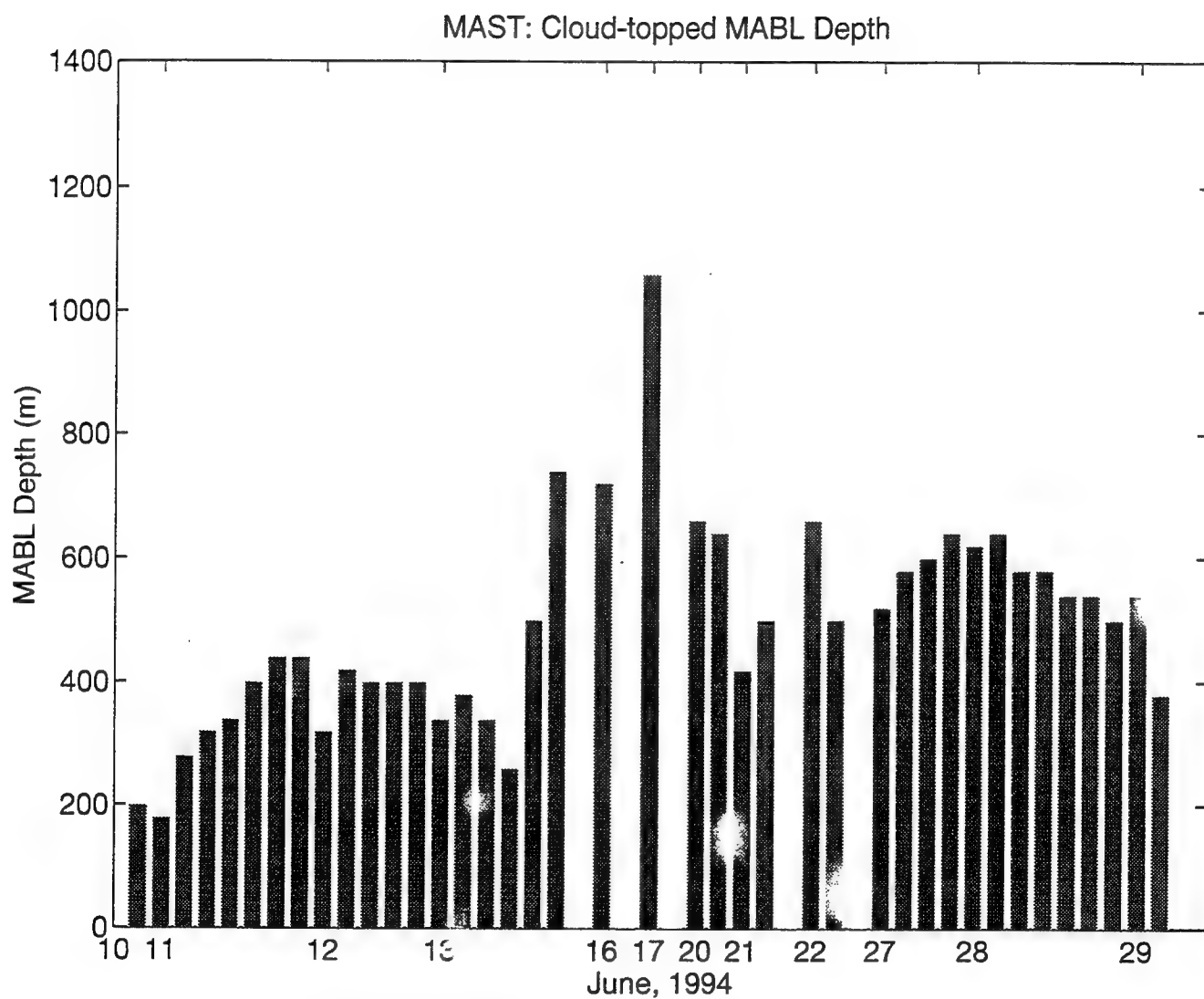
Figure 23. MABL depth for the 40 cloud-topped cases from MAST.

a. GL80

Sounding GL80 was launched at 1801 UTC on 27Jun94 at 35.40°N-124.84°W. R/V Glorita is well positioned within a track-rich environment in the corresponding satellite image, n9.94178.1752 (Figure 24). BL depth is 580 m. Figure 25 reveals the environment to be dry-adiabatic to the LCL at 977.3-mb (380 m), and moist through a cloud of thickness 200 m to the strong, very dry subsidence inversion. Cloud makes up 34.5% of the boundary layer depth.

SST (15.5°C) is warmer than the overlying air temperature (15.2°C). Surface winds are from the NW at 5 m/s. Wind data is not available for the boundary layer. Surface pressure is 1022.0-mb and relative humidity is 86.2%.

b. GL88

Sounding GL88 was launched at 1800 UTC on 28Jun94 at 35.33°N-124.07°W. R/V Glorita is again well positioned with respect to several shiptracks in the corresponding satellite image, n9.94179.1739 (Figure 26). BL depth is 540 m. Figure 27 reveals the environment to be dry-adiabatic (with some inhomogeneities) to the LCL at 976.2-mb (380 m) and moist through a cloud of thickness 160 m to the inversion base. Cloud makes up 29.6% of the boundary layer depth.

SST (14.6°C) is slightly cooler than the overlying air temperature (14.7°C). Winds are from the NNW at 7.5 m/s at the surface, decreasing in strength with height. Surface pressure is 1020.9-mb and relative humidity is 88.6%.

R/V Glorita logs indicate that drizzle was recorded during soundings GL86 and GL87, launched approximately six hours and three hours prior to this sounding.

c. Track-conducive Synopsis

For the 35 track-conducive cases for the MAST period, MABL depths are between 200 and 660 m. Again, clouds vary greatly with thickness, with drizzle detected on 2 occasions. SST is greater than the overlying air temperature on 20 occasions and air temperature is greater than the SST on six occasions. Air temperature is equal to SST for three cases and SST was not recorded in six instances. The air-sea temperature
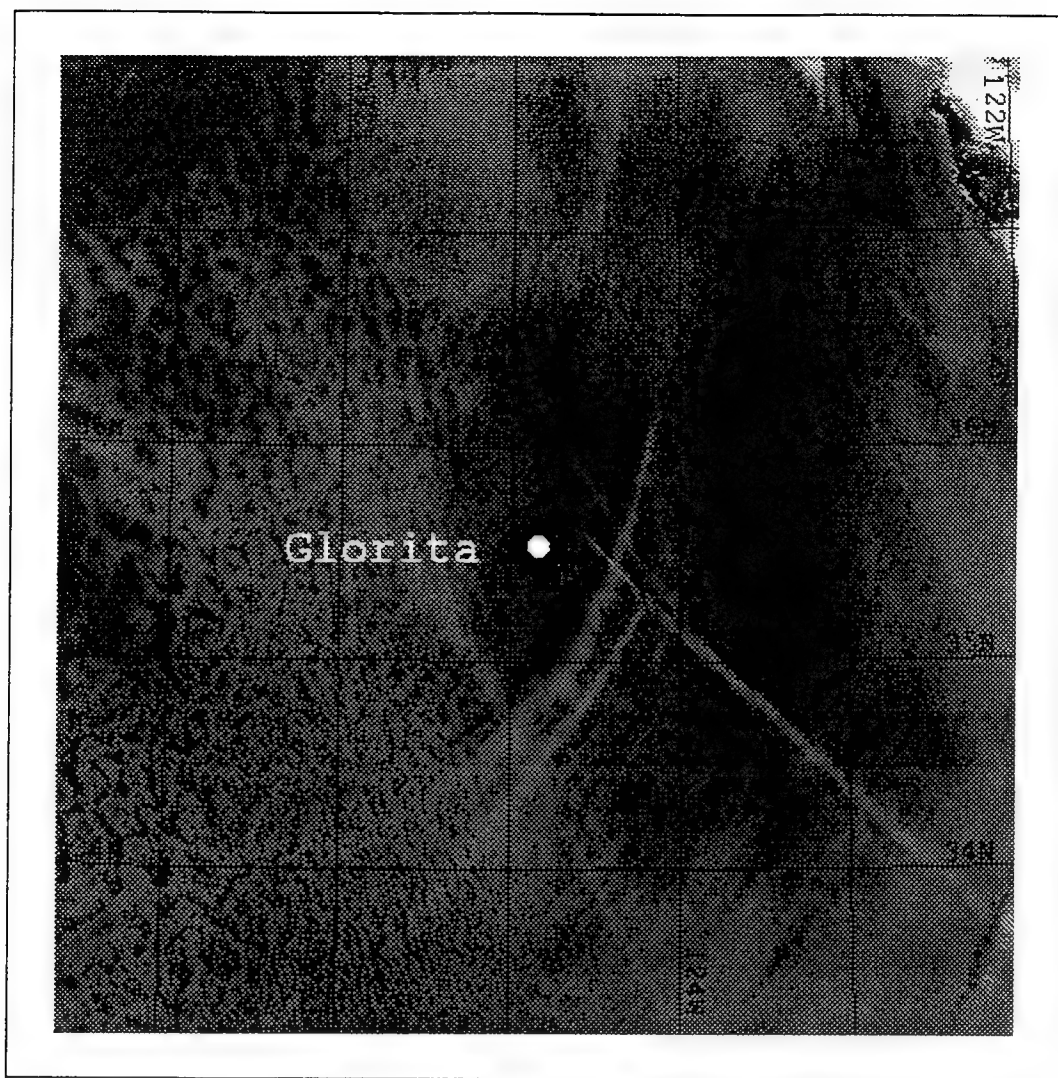
Figure 24. NOAA 9, AVHRR Channel 3 image from 27 June
1994, 1752 UTC. Location of R/V Glorita is indicated.
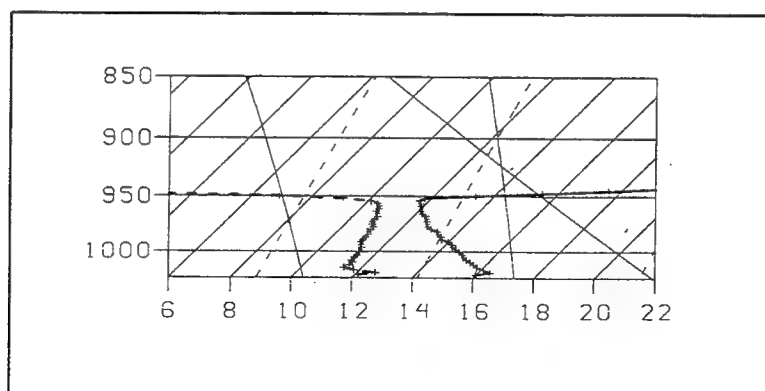
Figure 25. Sounding GL80, 27 June 1994, 1801 UTC.

42

Figure 26. NOAA 9, AVHRR Channel 3 image from 28 June 1994, 1739 UTC. Location of R/V Glorita is indicated.
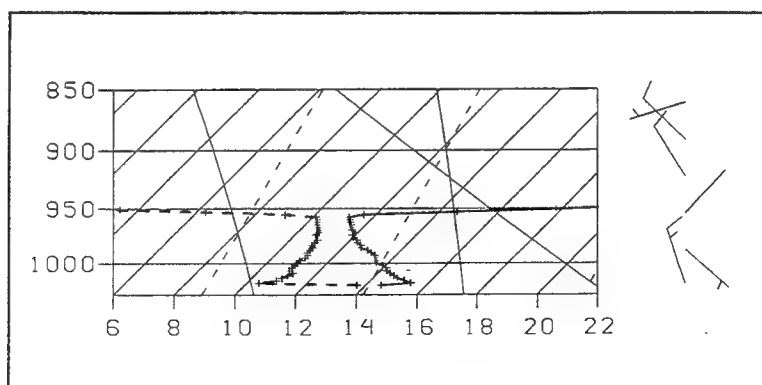
Figure 27. Sounding GL88, 28 June 1994, 1800 UTC.

difference is again small. Winds are from a generally northerly direction at the surface and vary in speed from near-zero to 12.3 m/s. Winds within the boundary layer were not accurate in most of the MAST dataset so they were not included in this study. Surface pressures are between 1015.0-mb and 1022.0-mb. Relative humidities are between 81.3% and 99.3%.

Table 6 displays information available relative to all track-conducive cases from MAST. Boundary layer depth is less than 700 m in all cases.

2. Non-track Cases

There were five instances from the MAST period where sounding/image pairs revealed that stratiform cloud was present in the boundary layer but there were no shiptracks observed. Table 7 lists pertinent information for these non-track cases. Two of these non-track cases will be presented as well as additional comments that may shed light on the nature of shiptracks.

a. GL13

Sounding GL13 was launched at 0252 UTC on 11Jun94 at 36.25°N-122.48°W. The corresponding image is n12.94162.0336 (Figure 28). Figure 29 reveals the environment to be stable to 1012.5-mb (20 m), dry-adiabatic to 1007.7-mb (60 m) and moist-adiabatic to 993.3-mb (180 m). Cloud thickness is 60 m making up 66.6% of the boundary layer depth.

SST was not recorded for this case. Air temperature is 13.4°C. Wind data is not available for this case. Surface pressure is 1014.5-mb and relative humidity is 96.5%.

Although the environment appears favorable and the boundary layer is shallow, there is a lack of shiptracks in the imagery. Larger scale dynamics have once again had an impact on shiptrack development. On the day prior to this sounding, a trough axis to the north shifted orientation to the west, allowing a southerly coastal surge of stratus clouds. The influence of continental aerosol sources on these clouds is evident in their high reflectance values. The MAST hypothesis requiring a low CCN background has been violated and thus these clouds are not susceptible to forcing by ship effluent. The role of continental aerosols in masking shiptracks is an area of active research.

44
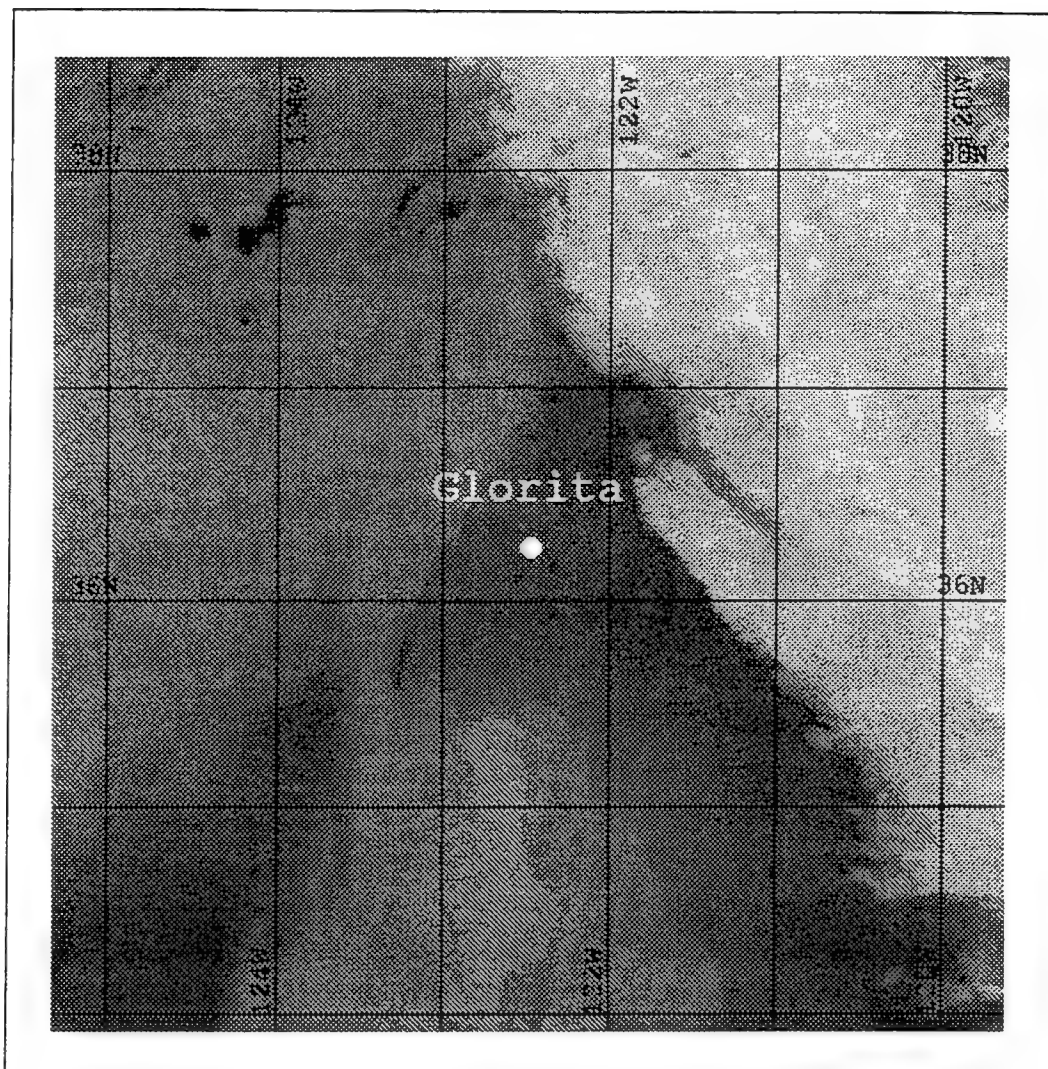
Figure 28. NOAA 12, AVHRR Channel 3 image from 11 June 1994, 0336 UTC. Location of R/V Glorita is indicated.
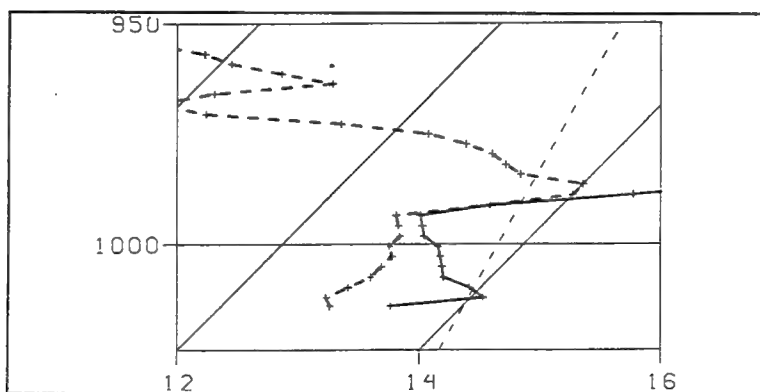
Figure 29. Sounding GL13, 11 June 1994, 0252 UTC.

45

b. GL36

Sounding GL36 was launched at 2338 UTC on 13Jun94 at 36.33°N-123.16°W. The corresponding image is n11.94165.0046 (Figure 30). Figure 31 reveals the atmosphere to be dry adiabatic to 972.9-mb (380 m) to an internal stable layer 40 m thick. The profile is again dry-adiabatic to the inversion at 931.7-mb (740 m). This sounding, taken approximately one hour prior to the satellite image, is in a region just north of the clouds in the image. The sounding was taken close enough to the cloud mass for the profile to be indicative of the cloudy air to the south. There are no shiptracks in these clouds. The presence of the decoupled boundary layer and a noticeable lack of shiptracks in these clouds supports the MAST hypothesis that an internal stable layer inhibits track production.

c. Additional Comments

A brief comment on one of the cases from MAST not featured in the text of thesis aids in understanding the complex nature of shiptracks.

- GL14: Suffers from continental aerosol effects (see GL13). This explains the lack of tracks on the shallow end of the distribution in Figure 30, to be discussed in the next paragraph.

3. MAST Summary

As in the SEAHUNT dataset, the MAST data reveals that shiptracks develop in shallow MABLs. Figure 32 is a histogram of the 40 cloud-topped MABLs from MAST. Shading indicates the occurrence of shiptracks. Again, shiptracks occur on the lower end of this distribution. The dataset suffers from a noticeable lack of non-track cases. The research vessel was generally either in a track-conducive regime or in cloud-free/broken cloud regions. It should be noted, however, that there were no conducive cases in this dataset where MABL depth exceeded 660 m. Again, this is strong evidence that shiptrack development is closely linked to boundary layer depth. No tracks were present in the continentally influenced stratus associated with the southerly surge. Also, no tracks were present in the one decoupled boundary layer found.

Figure 30. NOAA 11, AVHRR Channel 3 image from 14 June 1994, 0046 UTC. Location of R/V Glorita is indicated.
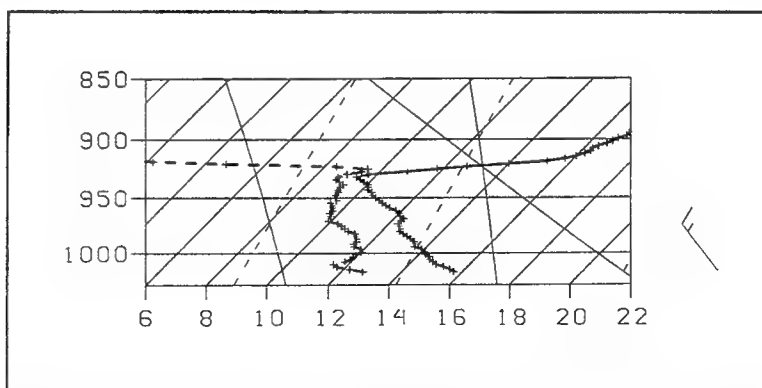
Figure 31. Sounding GL36, 14 June 1994, 2338 UTC.

MAST: Histogram of cloud-topped MABLs
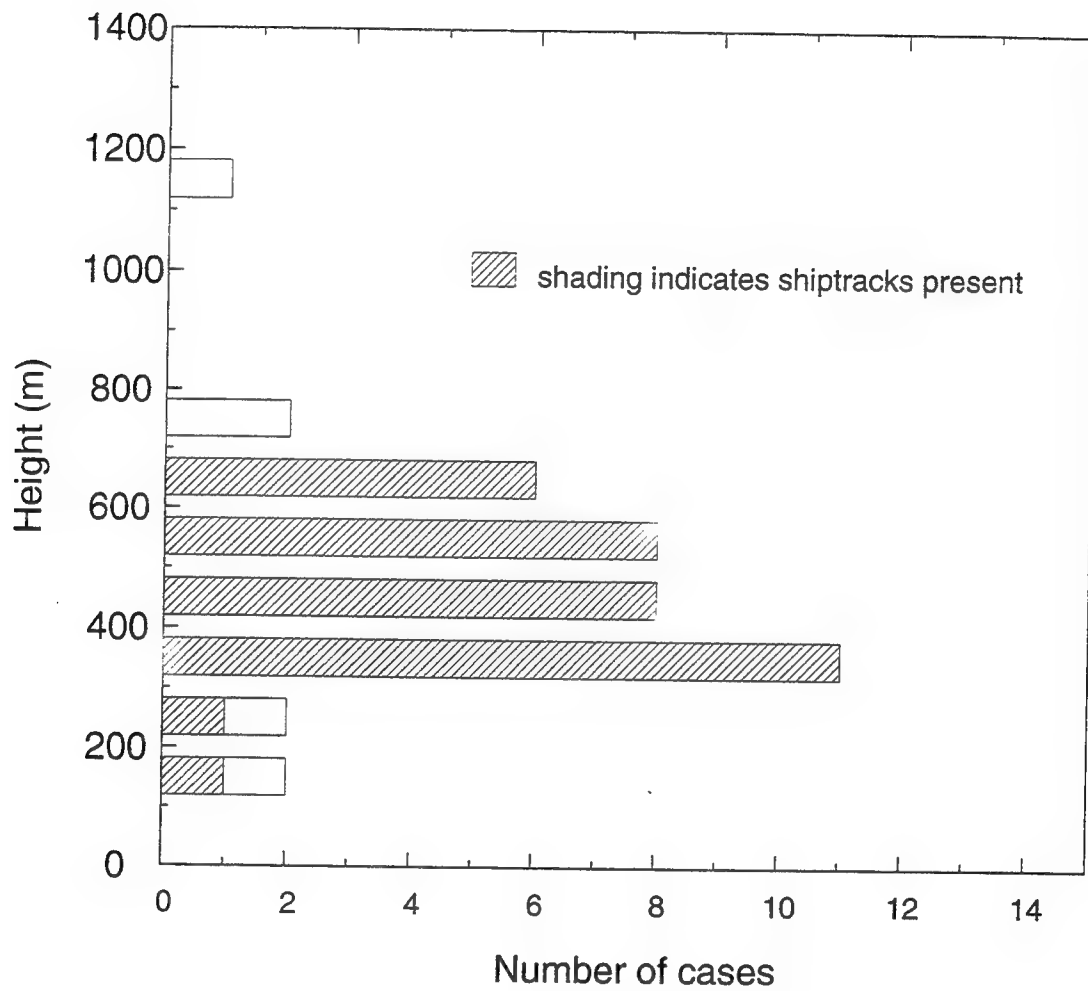
Figure 32. Histogram of all cloud-topped MABLs from MAST. Shading indicates the presence of shiptracks. No shiptracks were observed in boundary layers in excess of 700 m.

These observations support the MAST hypotheses regarding background environmental conditions necessary for the development and persistence of shiptracks.

C. COMPOSITE ANALYSIS

1. Boundary Layer Depth Analysis

Combining the datasets from both experiments provides a good foundation for a statistical analysis of shiptrack occurrence in the Californian stratus region. The two datasets complement each other well in that the SEAHUNT dataset has deeper boundary layers, on average, than the MAST set. This is attributed to the more southerly operating area for SEAHUNT. These deeper boundary layers are to be expected and are a direct result of the climatology presented in Chapter II.

Figure 33 is a histogram of boundary layer depth for the combined datasets. It demonstrates the occurrence of shiptracks in MABLs of depth between 180 and 716 m. No tracks were observed in MABLs deeper than this.

Figure 34 is a plot relating the occurrence of shiptracks to the non-occurrence of tracks. Both are plotted as a percent of occurrence for each bin in the histogram of Figure 31. The plot demonstrates that shiptracks occur in shallow boundary layers with peaks in the vicinity of 400 m. The non-occurrence profile (dashed line) has two peaks - one at 900 m and deeper and another around 200 m. The bimodal appearance in the non-occurrence profile is attributed to two factors. First, the lack of shiptracks in the deeper boundary layers supports the hypothesis of a required shallow MABL for shiptrack development. Secondly, the peak near 200 m is due to the influence of continental sources of aerosol in the shallow MABL of the coastal region (cases GL13, GL14) and the limited number of cases at that depth. The profiles overlap in the vicinity of 700 m (the edge of the track-conducive regime for this dataset).

2. An Updated Composite Environment

The availability of in situ data allows for an update to the work of Conover (1966), Bowley (1967), and Pettigrew (1992). Table 8 contains mean values of the shiptrack environment. It is similar in nature to that of Pettigrew (1992), Table 1, with
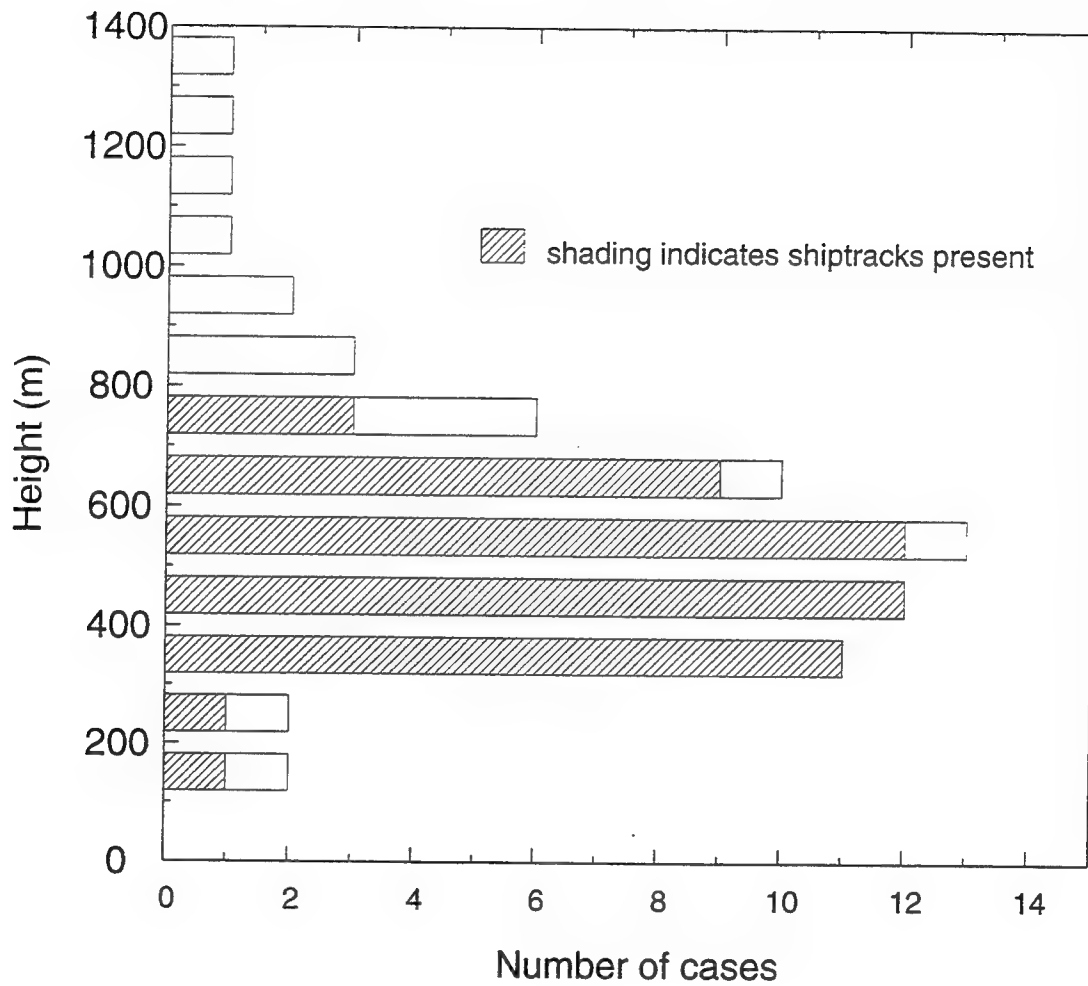
Figure 33. Composite histogram of all cloud-topped MABLs from both SEAHUNT and MAST. Shiptracks occur on the lower end of this distribution of BL depth.
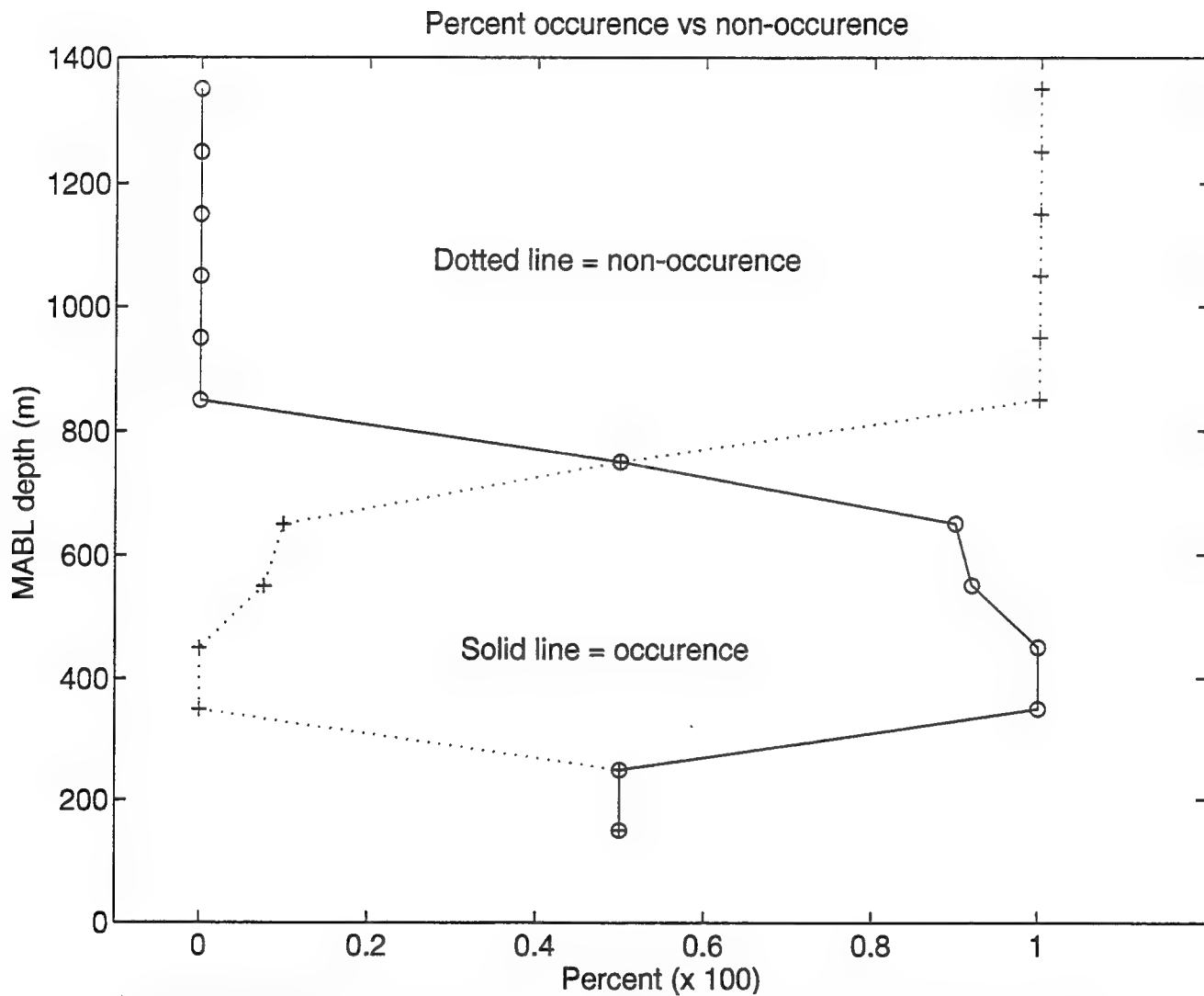
Figure 34. Percent occurence versus non-occurence of shiptracks for the combined dataset. Shiptracks were present in shallow boundary layers with peaks in the vicinity of 400m. The bimodal appearance of the non-occurence plot is due to both a decrease in shiptracks with height and the masking of shiptracks by continental sources of aerosol in the shallow boundary layers.

51

marked differences. As expected, this environment is characterized by high relative humidity, small air-sea temperature differences, and low to moderate northerly winds in a shallow cloud-topped MABL within a high pressure environment.

Primary differences between Table 8 and Table 1 are the inclusion of boundary layer depth and more precise measurement of the other variables. It is expected that since this analysis has been performed with values as determined by research vessels (as opposed to merchant ship weather reports), that the data better defines the true shiptrack environment.

Air and sea surface temperatures are in general agreement to previous findings but the mean air-sea temperature difference is negative for this dataset (vice positive as in Table 1), implying that SSTs are generally slightly warmer than the overlying air temperatures. This finding is not surprising. This is an expected result related to the climatology of the California stratus.

The addition of boundary layer depth to the shiptrack environment shows that tracks occurred between 200 and 716 m and had a mean of 504 ± 125 m. Winds were less variable in this dataset than in that used to construct Table 1.

3. The Non-Track Environment

Table 9 is a composite environment developed from the 16 non-track cloud-topped MABL cases. Note that the mean, minimum and maximum quantities for all surface variables are similar to those of the conducive environment. The primary difference between the non-track environment and the conducive environment is boundary layer depth. The mean MABL depth for the non-track cases is 812 ± 315 m. The large variability is due to the few cases of track-masking by continental-source aerosol. These cases also tend to lower the mean value and does not capture the bimodal nature of non-occurrence seen in Figure 34. The median value is slightly higher, 835 m, and slightly more indicative of the non-track environment of this small sample. The few shallow MABL non-track cases illustrate that while shiptrack development is highly dependent on boundary layer depth, the influence of background aerosol concentration is also quite significant in track development and detection.

4. Shiptrack Frequency Analysis

This analysis has revealed that shiptracks did not develop in boundary layers with depths exceeding 750 m. The next task is to determine if shiptracks decrease in frequency with increasing boundary layer depth, i.e., *Do clouds become less susceptible to the forcing associated with ship effluent as MABL depth increases?*

As described in Chapter III, individual tracks within 300 km and ± 0.5°C were counted for the conducive cases. From this data (195 shiptracks in all), a mean number of shiptracks versus MABL depth was plotted. MABL depth for the dataset was divided into 14 bins of width 99 m with tracks meeting selection criteria placed into the appropriate bin. For example, case EB06 has six shiptracks that are within the spatial and temperature restrictions imposed in this thesis. MABL depth is 580 m. A count of six is then placed in the 501-600 m bin. Non-track cases (in cloud-topped MABLs) contributed a count of zero to the appropriate bins. Once all tracks have been placed in their appropriate bin, a mean and standard deviation is determined for the bin and plotted at the midpoint of the bin. The mean number for the 501-600 m bin is plotted at 550 m, for example.

Figure 35 is a plot of mean shiptrack frequency versus MABL depth determined in this manner. It reveals that track development and persistence decreases with increasing boundary layer depth above 450 m for this dataset. There is a decrease in mean track frequency below 450 m. It is not suspected that shiptracks are less likely to develop in very shallow boundary layers. The following explanation is offered. It is important to note that MABL depth is shallowest in the coastal regime. MABL depths on the order of 300-400 m are common. Processing of sounding/image pairs in the coastal zone in the above manner is biased to low track numbers. The 512x512 m grids used in this analysis, overlap central and southern California when the research vessel is in the coastal zone, effectively excluding a portion of the grid from contributing any shiptracks for analysis. Furthermore, the shallow boundary layer of the coastal zone is more susceptible to the masking of shiptracks by aerosol of continental origin, decreasing the number of tracks detected there.

53
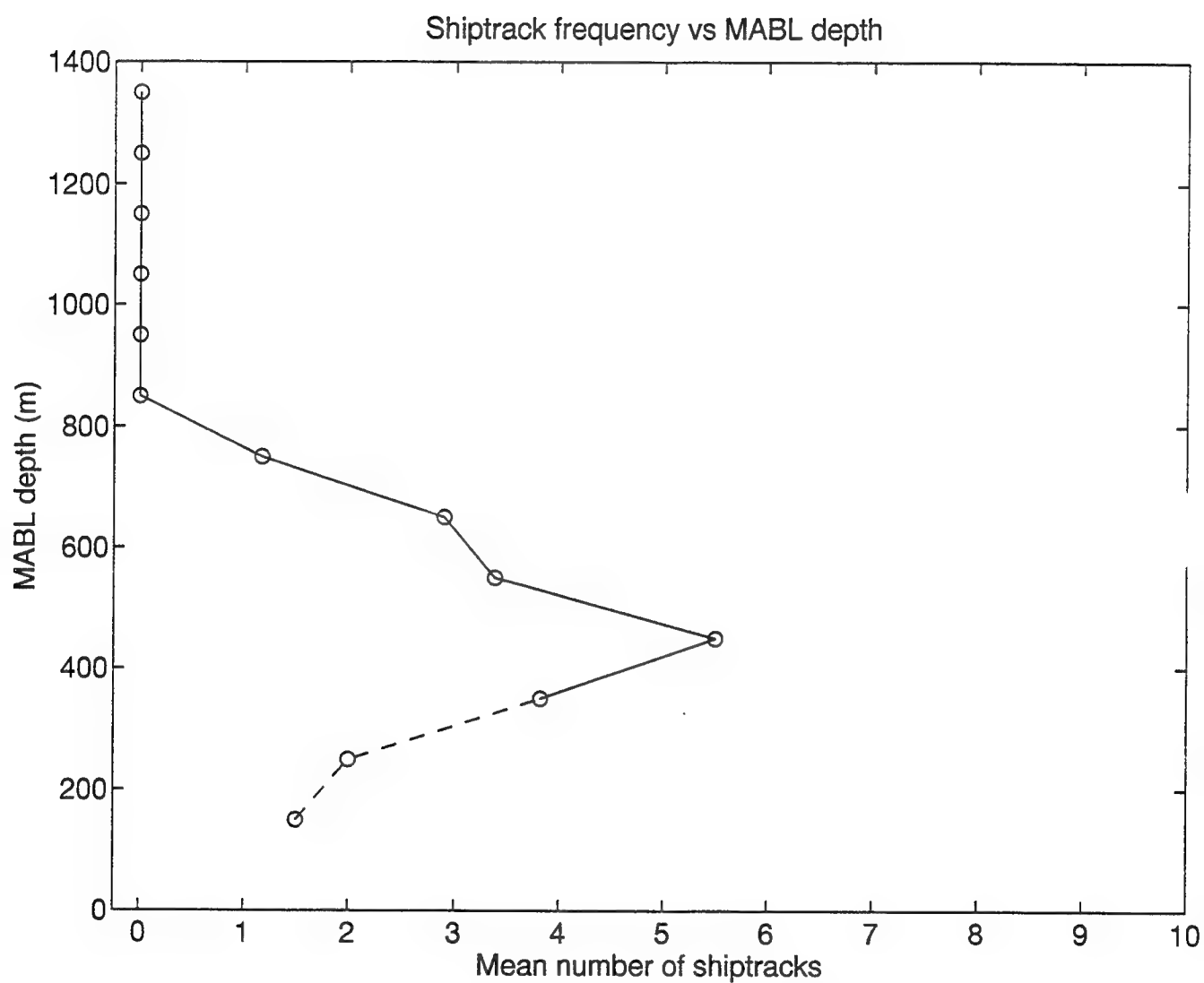
Figure 35. Plot of mean shiptrack frequency versus MABL depth. Above 400 m, frequency of shiptracks decreases with increasing boundary layer depth.

5. A Prototype Forecasting Tool

This analysis has demonstrated that shiptracks develop in shallow MABLs and decrease with increasing boundary layer depth. An obvious next step is to try to develop a means of determining and forecasting the probability of shiptrack development. This section proposes a prototype means of doing just that for the Californian stratus region.

Rosenthal and Helvey (1992) have demonstrated that boundary layer depth is related to the temperature difference between the base of the subsidence inversion (at cloud-top, or Tc) and that of the sea surface (SST). Increases in SST-Tc are associated with deeper marine boundary layers. Figure 36 is a scatter diagram of SST-Tc versus boundary layer depth for the combined dataset. As this temperature difference increases, so does boundary layer depth. Note that this profile closely parallels the dry-adiabat (solid line) in the figure. This is as expected, given that the environment in all cases is a relatively shallow, well-mixed marine boundary layer with thin to moderate cloud thicknesses associated with them.

Figure 37 is a superposition of the track frequency diagram (Figure 35) onto the scatter plot. Note that increases in SST-Tc are associated with increasing boundary layer depth and a decrease in the number of shiptracks. Thus, an ability to accurately determine the cloud-top and sea surface temperatures provides some ability to determine the likelihood of shiptrack occurrence. Preliminary analysis, for this limited sample in the Californian stratus region, indicates that a value for SST-Tc above 8°C indicates that it is unlikely to have shiptrack development.

As stated above, this is a suggested prototype shiptrack forecast tool. Recommendations for future development of this tool will be made in Chapter V.

D. PROPOSED MECHANISMS FOR OBSERVED PHENOMENON

There are several mechanisms that may explain why the frequency of shiptracks decreases with increasing MABL depth. Based on the evaluation of this dataset, a
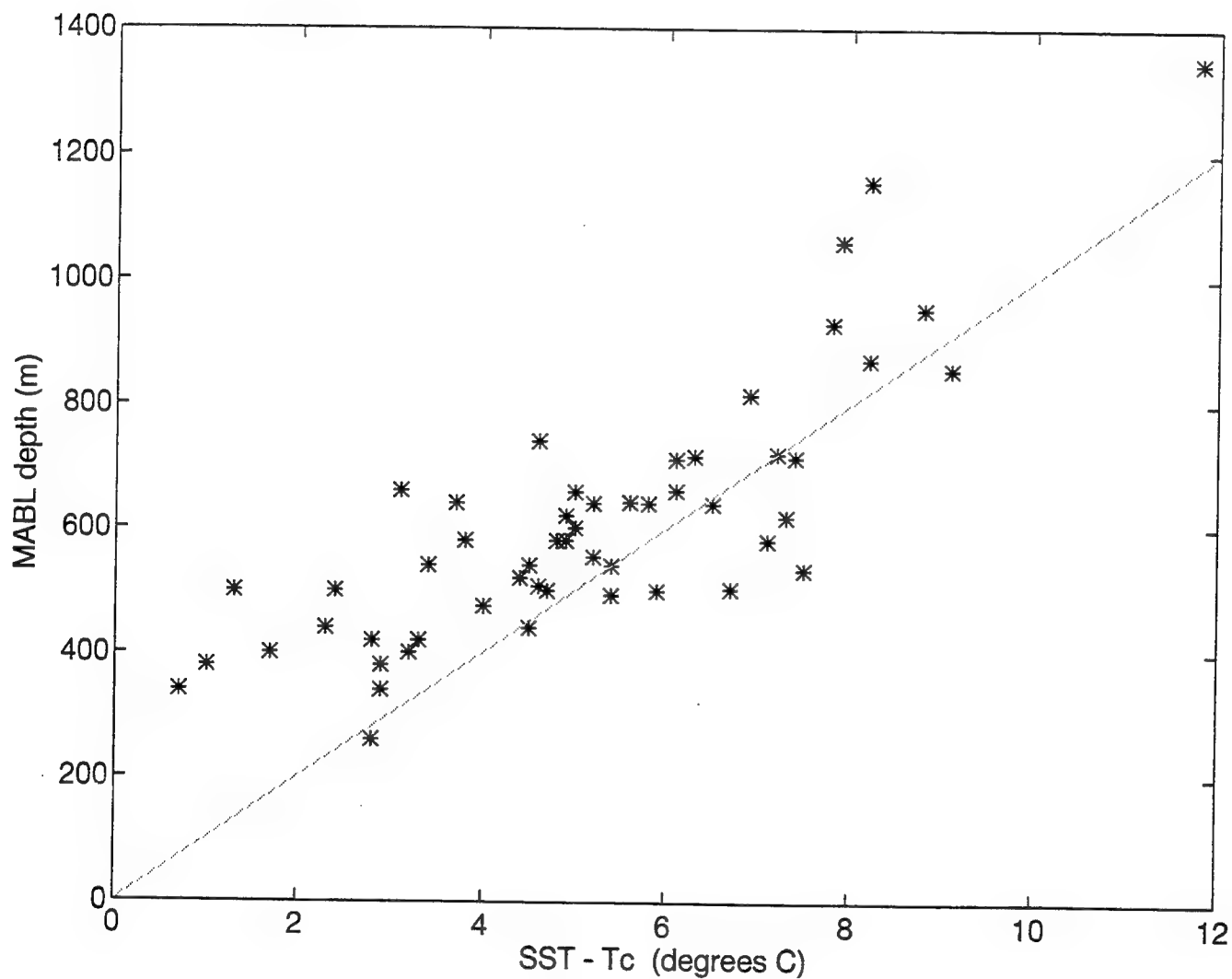
Figure 36. Scatter diagram of the temperature difference between the sea surface (SST) and cloud-top temp (Tc). (SST-Tc) increases with increasing boundary layer depth.
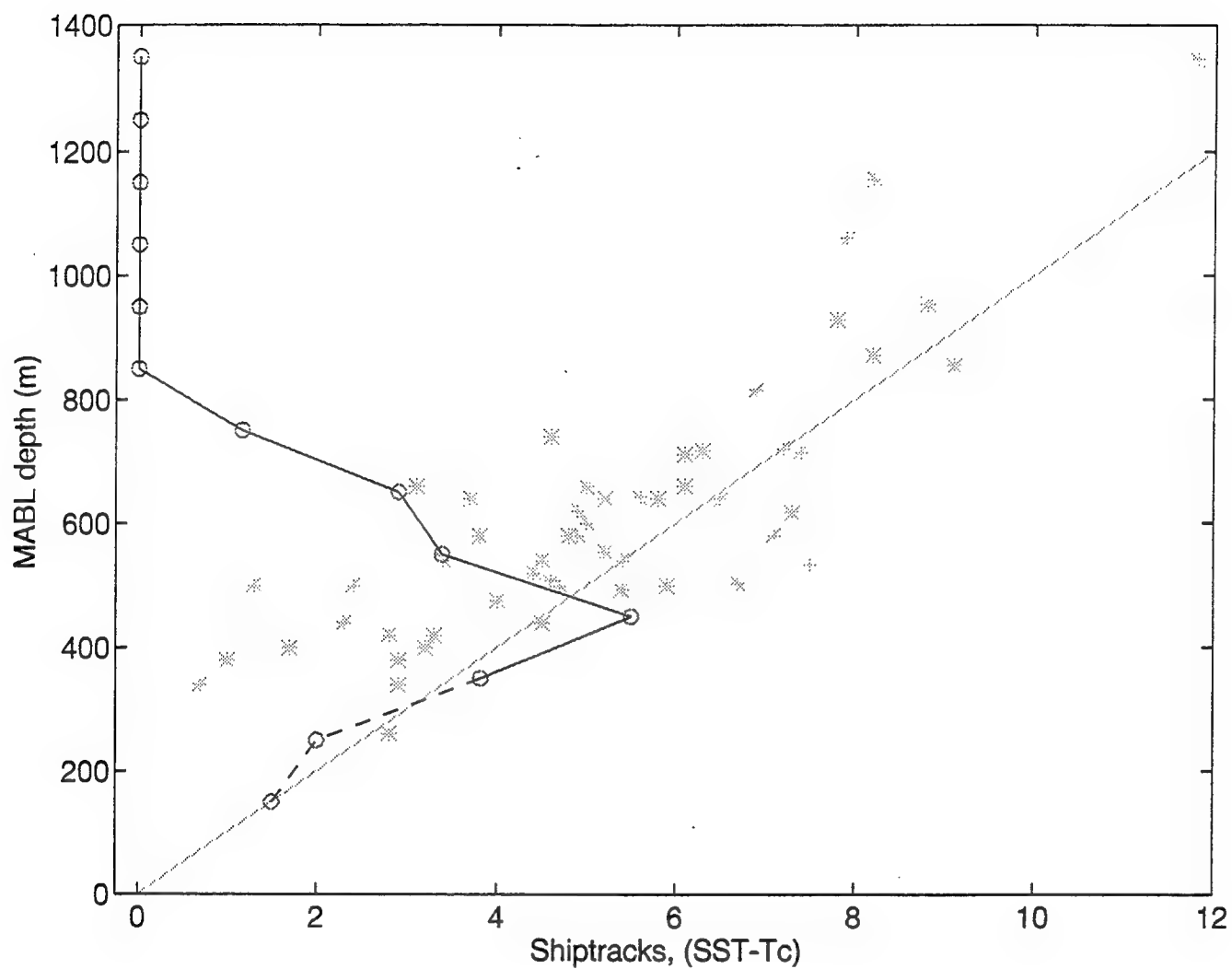
Figure 37. Prototype Shiptrack Forecasting Tool. Y axis is MABL depth. X axis is both the mean number of shiptracks and SST-Tc (°C).

conjecture is that there may exist at least two types of threshold that explain why shiptracks do not develop in deep boundary layers. These can be divided into the following categories:

- Detection Threshold

- Physical Threshold

1. Detection Threshold

The marine boundary layer deepens due to enhanced vertical mixing and entrainment of dry air. It is reasonable to expect that the deeper the boundary layer, the greater likelihood there is for ship effluent to disperse over a greater volume prior to reaching cloud base. Additionally, this dispersion is accompanied by the entrainment of dry air. Both would act to dilute ship-produced aerosol.

Figure 38 illustrates this concept. MABL-1 has a depth of 700 m. A cross-section of MABL-1 shows an eddy, transporting air parcels in this well mixed environment. The cross-sectional area of MABL-1 is 490,000 m^2 (700x700 m). A 300 m increase in MABL depth to 1000 m (a 42.8% increase) yields a 104% increase in the cross-sectional area (from 490,000 m^2 to 1,000,000 m^2). Thus a slight increase in MABL depth has resulted in a much larger area of circulation and the likelihood of dilution of the ship-effluent. The less effluent that reaches cloud base, the lower the increase in reflectivity at 3.7 μm will be. CCN concentrations that cause only a slight brightening of cloud will not be discernable if the brightness increase is below the radiometric resolution of AVHRR Channel 3. Future improvements in sensor resolution will resolve this issue.

2. Physical Threshold

Shiptracks are a result of enhanced reflectivity of cloud due to regions of smaller, highly concentrated drops. As the ship-generated aerosol is dispersed over a broader range throughout this deeper MABL, the number of CCN per cm^3 will decrease. As this happens, the decreasing droplet size associated with increasing CCN will be altered. There may be a critical value of aerosol concentration needed to produce the required droplet
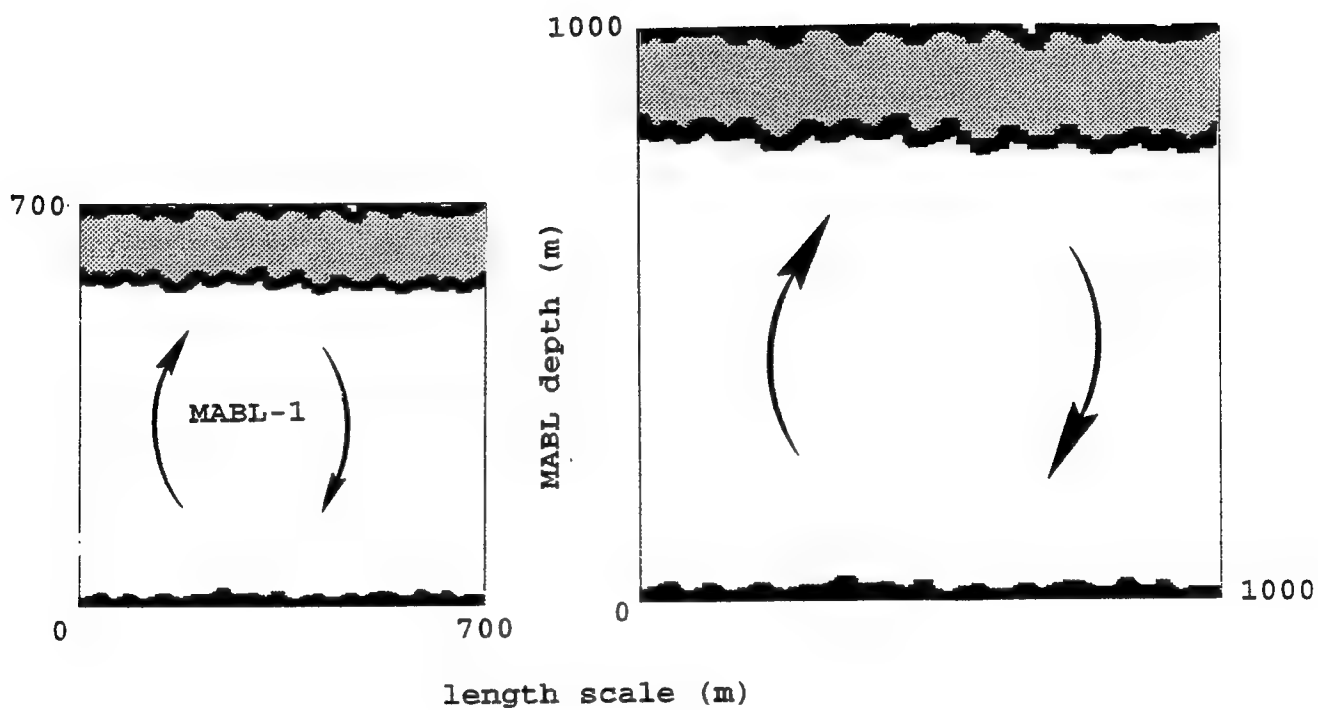
Figure 38. Highly schematic diagram to show how changes
in boundary layer depth may significantly impact the size
of circulation eddies, leading to greater dispersion of
anthropogenic aerosol and a decrease in shiptracks.

size distribution for shiptrack formation. The basic question here is: *How much anthropogenic aerosol is required per cm^3 to cause the significant change in droplet size distribution and corresponding increase in reflectivity necessary to produce a shiptrack? Detailed studies relating changes in cloud microphysics to the corresponding change in radiative properties that those microphysical modifications cause, are necessary.

V. CONCLUSIONS AND RECOMMENDATIONS

A. CONCLUSIONS

The purpose of this thesis was to test several hypotheses of the MAST experiment through the analysis of data from two experiments, SEAHUNT and MAST. Sounding/image pairs for 65 cloud-topped marine boundary layers were analyzed for the occurrence and non-occurrence of shiptracks. The primary result is the demonstration that shiptrack development and persistence is highly dependent on the presence of a shallow-cloud-topped MABL.

Analysis of the SEAHUNT, MAST, and composite datasets revealed that shiptracks were found in environments of boundary layer depth less than 750 m. It was shown that, in a distribution of cloud-topped MABLs, shiptracks occurred on the low (shallow) end of the distribution.

Analyses revealed that frequency of occurrence versus non-occurrence of shiptracks have distinct peaks. The occurrence distribution had a peak at boundary layer depths from 400-500 m. The non-occurrence frequency distribution was bimodal in nature due to two processes. A peak at 900 m and above is indicative of the decrease in shiptracks with increasing boundary layer depth. The peak near a boundary layer depth of 200 m was due to masking of shiptracks by continental-source aerosol. While the latter aids in validating the MAST hypothesis for a required low CCN background, it additionally demonstrates the complexity in predicting the likelihood of shiptrack development.

Composite environments for track-conducive and non-track regimes were presented as well. Analysis reveals that surface parameters are similar in cases of occurrence and non-occurrence of shiptracks and are not different from the climatological values of the Californian stratus. The primary difference between the track and non-track environment was boundary layer depth. Above a boundary layer depth of 450 m, the frequency of shiptrack occurrence decreased with increasing depth, providing additional evidence that

61

boundary layer depth is a key environmental parameter in track development and detection.

Mechanisms were proposed to explain the observed decrease in number of shiptracks with increasing boundary layer depth. These proposed mechanisms take into account the role of both a detection threshold and a physical threshold in shiptrack production. The development and persistence of shiptracks is an extremely complicated process and the occurrence of tracks is likely related to a combination of both mechanisms.

B. RECOMMENDATIONS

Although shiptracks were not observed with boundary layer depths in excess of 750 m, it is likely that, under proper conditions, they can develop in deeper boundary layers. This analysis was dependent on the location of the research vessels for the two field experiments. Due to logistical considerations (food, crew swaps), these vessels are restricted in how far seaward they can go. Shiptracks are often observed in the stratiform clouds further west than the SEAHUNT and MAST operating areas where boundary layer depths are generally greater. While this is true, it is expected that the same trend in decreasing track number versus boundary layer depth will hold true. Future track studies using these analysis techniques are needed to confirm this. Additionally, a weighting of the satellite image for amount of susceptible cloud cover is likely to reveal that MABLs of depths less than 450 m are not less likely to be susceptible to track production as might be construed from the shape of the shiptrack frequency diagram.

While this analysis used sounding/image pairs from two experiments designed to study shiptracks, there is no reason it cannot be supplemented, using a combination of ocean based soundings and corresponding imagery from any period of time. The creation of a database of sounding/image pairs using sounding data from deployed Navy meteorological teams and ships, research expeditions, aircraft profiles, and the corresponding satellite imagery, is required to give this phenomenon adequate statistical treatment.

This study did not focus on particular propulsion plant types in the analysis. It is conceivable that shiptrack frequency diagrams versus MABL depth can be created for each class of fuel/propulsion type. Fossil fuel plants are suspected of making the bulk of the shiptracks observed. It is likely that cleaner-burning propulsion plants leave shiptracks only in the shallowest boundary layers and that the so-called "dirty burners" are more likely to leave a shiptrack in the deeper boundary layers. Detailed analysis of both stack emissions and the chemistry of shiptracks is required to confirm what types of ships are most likely to cause shiptracks.

There are several avenues to pursue in the development of the shiptrack forecast tool. This document is an analysis of all shiptracks that met the spatial and temperature criteria of the thesis. As noted above, future studies in fuel/engine types most associated with track development may lead to the development of a set of shiptrack frequency curves - each dependent on ship propulsion type. Additionally, probability diagrams may be developed for varying degrees of background CCN. Given the complex nature of shiptrack development, it is not believed that one curve will be sufficient in the forecasting of shiptracks. Also, the shiptrack frequency curve can be extended to other regions of the world, each with it own differing climatologies that will effect the shape of the curves.

Remote sensing techniques should be employed in determining cloud-top temperatures that, when combined with a ship reported SST, may be used to determine boundary layer depth and the probability of shiptracks. Rosenthal and Helvey (1992) have discussed the feasibility of this technique in regards to determining surface duct heights and their technique will be employed in the next version of the Navy's TESS. Their technique is directly transferable to the boundary layer depth/shiptrack forecast problem.

This thesis is the first critical analysis of data from the MAST experiment. The dataset used for this analysis represents just a fraction of the abundance of information collected during the experiment. Atmospheric profiles from MAST aircraft and soundings from Navy ships operating in the MAST area are forthcoming and should be added to this analysis as they become available.

63

APPENDIX A. TABLES

This appendix serves as a convenient location to consolidate the tables discussed in the text of this thesis.

.

.

	mean	minimum	maximum
Surface Pressure (mb)	1021.1	1014.8	1027.2
Ta (°C)	18.9	13.0	21.0
Tw (°C)	18.2	12.0	21.0
Ta-Tw (°C)	0.8	-4.0	4.0
True wind speed (m/s)	6.8	3.0	26.0
sky cover St/Sc (octas)	7.6	3.0	8.0

Table 1. Composite surface meteorological parameters of the shiptrack conducive environment. After Pettigrew (1992).

Sounding Number	Launch Time (date - UTC)	Corresponding Satellite Image (date: sat: UTC)	Analysis
EB01	11Jul - 1215	11Jul; n11; 1112	Conducive
EB02	- 1700	none	Dismissed - no image
EB03	- 1820	none	Dismissed - no image
EB04	- 1900	none	Dismissed - no image
EB05	12Jul - 0000	11Jul; n11; 2230	Conducive
EB06	- 1200	12Jul; n11; 1101	Conducive
EB07	13Jul - 0000	n11; 2219	Dismissed - bad sounding
EB08	- 1200	13Jul; n11; 1048	Conducive
EB09	- 2020	; n11; 2210	Conducive
EB10	14Jul - 0000	; n11; 2210	Conducive
EB11	- 1200	14Jul; n11; 1036	Conducive
EB12	15Jul - 0000	n11; 2158	No Tracks
EB13	16Jul - 1200	16Jul; n11; 1154	No tracks
EB14	17Jul - 0000	n11; 2134	Dismissed - bad sounding
EB15	- 1200	17Jul; n11; 1143	Conducive
EB16	18Jul - 0000	n11; 2123	No Tracks
EB17	- 1215	18Jul; n11; 1132	No Tracks
EB18	19Jul - 0000	n11; 2252	No Tracks
EB19	- 1200	19Jul; n11; 1119	No Tracks

Table 2. SEAHUNT experiment soundings, corresponding satellite image and environmental analysis. An analysis of *conducive* indicates that there was at least one shiptrack that met the selection criteria specified in the thesis.

Table 2 continued.

EB20	20Jul - 0000	n11: 2240	No Tracks
EB21	- 1200	20Jul: n11: 1107	No Tracks
EB22	21Jul - 0000	n11: 2229	No Tracks
EB23	- 1200	21Jul: n11: 1050	No tracks
EB24	23Jul - 1315	23Jul: n11: 1034	No Tracks
EB25	24Jul - 1200	24Jul: n11: 1203	Conducive
EB26	25Jul - 0000	n11; 2144	Conducive
EB27	- 0210	none	dismissed - no image
EB28	- 1200	25Jul: n11; 1151	Conducive
EB29	26Jul - 0000	n11; 2132	Conducive
EB30	- 1200	26Jul; n11; 1148	Conducive
EB31	27Jul - 0000	n11; 2302	Dismissed - broken cloud
EB32	- 1220	27Jul; n11: 1128	Conducive
EB33	28Jul - 0000	n11; 2251	Dismissed - clear air

Sounding Number	MABL Depth (m)	% of MABL that is cloud	Ta-Ts (°C)	Sfc Pressure (mb)	RH	Surface Wind Data dir-spd(m/s)
EB01	716	59.6	0.4	1015.7	78	000 - 3.4
EB05	708	29.0	(-)	1016.7	79	010 - 3.4
EB06	580	31.7	-0.8	1017.9	86	000 - 7.7
EB08	493	(-)	-0.8	1018.4	99	350 - 7.7
EB09	470	36.1	(-)	1019.3	83	330 - 9.8
EB10	554	45.5	0.1	1017.6	90	340 - 7.7
EB11	507	77.9	0.0	1014.3	98	345 - 6.2
EB15	711	21.5	0.9	1019.2	85	290 - 5.0
EB25	658	78.4	0.5	1016.7	93	320 - 7.7
EB26	475	44.0	1.5	1016.8	80	330 - 11.3
EB28	496	53.0	(-)	1015.0	92	330 - 10.3
EB29	642	41.2	0.6	1015.3	90	315 - 10.3
EB30	639	57.1	-0.4	1015.0	78	315 - 2.6
EB32	503	26.6	-2.4	1017.9	72	320 - 2.1

Table 3. SEAHUNT track-conducive environmental data. A (-) symbol indicates missing data.

Sounding Number	MABL depth (m)	% of MABL that is cloud	Ta-Ts (°C)	Sfc Pressure (mb)	RH	Surface Wind Data dir-spd(m/s)
EB12	533	23.1	-0.6	1014.4	79	350-1.0
EB13	714	31.8	0.6	1018.0	78	230-2.6
EB16	856	23.0	0.0	1019.6	70	310-5.1
EB17	1346	45.2	0.0	1018.4	71	340-5.1
EB18	929	(*)	1.0	1017.6	62	000-7.7
EB19	953	51.3	-0.9	1017.1	86	330-8.5
EB20	1225	8.7	(-)	1016.4	72	330-7.2
EB21	1155	53.6	-0.1	1015.5	95	310-6.2
EB22	871	25.3	1.3	1017.0	72	045-1.5
EB23	815	47.1	0.5	1016.8	85	310-1.5
EB24	61	69.5	-1.4	1016.0	92	310-4.0

Table 4. SEAHUNT Non-track cases. A (-) symbol indicates missing data. (*) indicates indistinct LCL.

Sounding Number	Launch Time (date - UTC)	Corresponding Satellite Image (date: sat; UTC)	Analysis
GL01	3Jun - 0029	none	Dismissed - test sounding
GL02	5Jun - 2357	6Jun; n11; 0043	Dismissed - clear air
GL03	6Jun - 1447	n11; 1537	Dismissed - broken cloud
GL04	- 2039	none	Dismissed - no image
GL05	8Jun - 0535	8Jun; n12; 0302	Dismissed - clear air
GL06	- 1149	n11; 1244	Dismissed - clear air
GL07	- 1737	n11; 1521	Dismissed - broken cloud
GL08	- 2353	9Jun; n11; 0006	Dismissed - broken cloud
GL09	10Jun - 1739	10Jun; n12; 1617	Dismissed - clear air
GL10	- 1929	n12; 1810	Dismissed -no MABL clouds
GL11	- 2058	none	Dismissed - no image
GL12	- 2354	n11; 2342	Conducive
GL13	11Jun - 0252	n12; 0336	No tracks
GL14	- 0549	n9; 0533	No tracks
GL15	- 0838	none	Dismissed - bad sonde
GL16	- 1153	n11; 1347	Conducive
GL17	- 1448	n10; 1516	Conducive
GL18	- 1746	n9; 1757	Conducive
GL19	- 2041	n9; 2330	Conducive

Table 5. MAST experiment soundings, corresponding satellite image and analysis.

Table 5 continued.

GL20	- 2343	12Jun; n10; 0054	Conducive
GL21	12Jun - 0244	n12; 0315	Dismissed - clear air
GL22	- 0541	n9; 0517	Dismissed - clear air
GL23	- 1146	n11; 1335	Conducive
GL24	- 1448	none	Dismissed - bad sonde
GL25	- 1732	n12; 1534	Conducive
GL26	- 2020	n9; 1741	Conducive
GL27	- 2132	13Jun; n11; 0058	Conducive
GL28	- 2347	n11; 0058	Conducive
GL29	13Jun - 0242	n12; 0253	Conducive
GL30	- 0549	n9; 0508	Conducive
GL31	- 0841	none	Dismissed - no image
GL32	- 1143	n11; 1322	Conducive
GL33	- 1451	n12; 1512	Conducive
GL34	- 1741	n12; 1652	Conducive
GL35	- 2030	none	Dismissed - no image
GL36	- 2338	n11; 0046	No tracks - decoupled
GL37	14Jun -0242	14Jun; n12; 0231	Dismissed - clear air
GL38	- 0537	n9; 0455	Dismissed - clear air
GL39	15Jun -1740	n9; 1705	Dismissed - clear air
GL40	- 2324	15Jun; n11; 0020	Dismissed - clear air
GL41	16Jun - 0257	n12; 0327	Dismissed - clear air
GL42	- 0542	n9; 0427	Dismissed - clear air
GL43	- 1145	n11; 1244	No tracks

Table 5 continued.

GL44	- 1456	n11; 1426	Dismissed - broken cloud
GL45	- 1735	16Jun; n9; 1652	Dismissed - broken cloud
GL46	- 2030	none	Dismissed - no image
GL47	- 2335	none	Dismissed - no image
GL48	17Jun -0244	17Jun; n12; 0307	Dismissed - broken cloud
GL49	- 0545	n9; 0416	Dismissed - poor image
GL50	- 0841	none	Dismissed - no image
GL51	- 1156	n11; 1233	Dismissed - broken cloud
GL52	- 1448	n11; 1414	No tracks
GL53	- 1804	n9; 1820	Dismissed - clear air
GL54	18Jun - 0000	n11; 2357	Dismissed - clear air
GL55	20Jun - 1458	n10; 1459	Conducive
GL56	- 1809	n9; 1741	Conducive
GL57	- 2358	21Jun; n11; 0101	Dismissed - clear air
GL58	21Jun - 0233	n12; 0320	Dismissed - clear air
GL59	- 0551	n9; 0505	Dismissed - poor image
GL60	- 0847	none	Dismissed - no image
GL61	- 1150	n11; 1325	Dismissed - sunglint
GL62	- 1503	n12; 1539	Conducive
Gl63	- 1751	n9; 1729	Conducive

Table 5 continued.

GL64	- 2053	none	Dismissed - no image
GL65	- 2352	22Jun; n11; 0048	Dismissed - clear air
GL66	22Jun -0244	n12; 0259	Dismissed - clear air
GL67	- 1148	n11; 1312	No tracks
GL68	- 1453	n12; 1518	Conducive
GL69	- 1752	n12; 1716	Conducive
GL70	- 2046	none	Dismissed - no image
GL71	- 2346	23Jun; n11; 0036	Dismissed - clear air
GL72	23Jun -0249	n12; 0239	Dismissed - clear air
GL73	- 0545	n9; 0439	Dismissed - clear air
GL74	- 2006	none	Dismissed - clear air
GL75	26Jun - 0546	26Jun; n12; 0312	Dismissed - clear air
GL76	- 1453	n12; 1532	Dismissed - clear air
GL77	- 2151	n11; 2346	Dismissed - no MABL clouds
GL78	27Jun -0241	27Jun; n11; 0127	Dismissed - no MABL clouds
GL79	- 1452	n12; 1510	Conducive
GL80	- 1801	n9; 1752	Conducive
GL81	- 2053	n9; 1752	Conducive
GL82	- 2349	n11; 2334	Conducive
GL83	28Jun - 0238	28Jun; n12; 0228	Conducive
GL84	- 0545	n9; 0515	Conducive
GL85	- 0855	none	Dismissed - no image
GL86	- 1150	n11; 1340	Conducive
GL87	- 1451	n10; 1507	Conducive

Table 5 continued.

GL88	- 1800	n9; 1739	Conducive
GL89	- 2057	n9; 1739	Conducive
GL90	- 2344	29Jun: n11; 0102	Conducive
GL91	29Jun - 0249	n12: 0207	Conducive
GL92	- 0547	none	Dismissed - no image
GL93	- 0841	none	Dismissed - no image
GL94	- 1645	n9; 1726	Conducive

Sounding Number	MABL depth (m)	% of MABL that is cloud	Ta-Ts (°C)	Sfc Pressure (mb)	RH	Surface Wind Data dir-spd(m/s)
GL12	200	60.0	(-)	1015.0	95.5	159-6.0
GL16	320	75.0	(-)	1015.0	98.8	281-0.3
GL17	340	88.2	(-)	1015.5	99.3	191-1.3
GL18	400	70.0	-0.8	1017.0	99.0	152-3.2
GL19	440	81.8	-0.5	1016.3	97.4	184-2.9
GL20	440	63.6	-1.9	1016.5	93.3	319-6.1
GL23	320	(-)	(-)	1016.6	94.0	330-12.0
GL25	420	61.9	-0.2	1016.7	95.5	321-10.2
GL26	400	55.0	(-)	1017.7	93.2	319-8.9
GL27	400	65.0	(-)	1017.2	94.0	318-10.3
GL28	400	45.0	-0.8	1017.0	94.7	308-10.7
GL29	340	23.5	-0.6	1016.8	91.9	312-7.0
GL30	380	42.0	0	1016.5	90.7	328-7.1
GL32	340	76.4	0.7	1015.8	97.0	336-8.1
GL33	260	76.9	-1.4	1016.0	98.6	336-9.3
GL34	500	(-)	-0.9	1017.0	99.0	334-8.5
GL55	660	51.5	0.2	1019.8	95.2	338-4.1
GL56	640	28.1	0.3	1021.0	89.9	342-5.8
GL62	420	23.8	0	1019.9	87.7	339-11.2
GL63	500	28.0	1.8	1020.5	84.7	328-7.5
GL68	660	36.4	-1.1	1021.1	84.4	334-9.0
GL69	500	(-)	-0.9	1021.9	81.3	344-8.3
GL79	520	34.6	-0.8	1020.8	86.5	346-9.6

Table 6. MAST track-conducive environmental data. A (-) indicates missing data.

Table 6 continued.

GL80	530	34.5	-0.3	1022.0	86.2	342-9.7
GL81	600	20.0	-0 2	1022.0	84.4	342-9.6
GL82	640	34.3	0	1021.8	83.8	346-8.9
GL83	520	29.0	-0.5	1020.8	85.4	338-10.2
GL84	540	34.3	-0.6	1021.9	87.9	335-9.4
GL86	580	41.3	-0.7	1019.1	89.9	343-9.6
GL87	580	51.7	-0.5	1019.5	90.3	349-9.1
GL88	540	25.9	0.1	1020.9	88.6	348-8.7
GL89	540	33.3	-0.5	1021.8	85.4	359-10.4
GL90	500	20.0	-0.8	1021.9	86.7	358-11.5
GL91	540	33.3	-1.2	1021.9	88.5	353-9.2
GL94	380	57.9	0.8	1019.0	93.2	339-12.3

Sounding Number	MABL depth (m)	% of MABL that is cloud	Ta-Ts (°C)	Sfc Pressure (mb)	RH	Surface Wind Data dir-spd(m/s)
GL13	180	66.6	(-)	1014.5	96.5	252-0.9
GL14	280	42.9	(-)	1015.5	99.2	347-5.0
GL36	740	56.7	0.6	1017.5	90.1	327-8.9
GL43	720	33.3	-0.9	1020.8	80.3	350-11.5
GL52	106ι.	32.1	0.4	1022.8	80.8	335-11.7

Table 7. MAST non-track cases. A (-) symbol indicates missing data.

	mean	minimum	maximum
Boundary Layer Depth (m)	504 ± 125	200	716
Ta (°C)	14.6 ± 1.9	11.2	19.9
SST (°C)	14.9 ± 1.7	11.0	19.0
Ta-SST (°C)	-0.3 ± 0.8	-2.4	1.8
Surface Pressure (mb)	1018.3 ± 2.4	1014.3	1022.0
Relative Humidity (%)	89.7 ± 6.5	72	99.3
% of MABL that is cloud	46.9 ± 19.3	20.0	88.2
True Wind Speed (m/s)	7.8 ± 3.0	0.3	12.3

Table 8. The composite shiptrack environment.

	mean	minimum	maximum
Boundary Layer Depth (m)	812 ± 316	180	1346
Ta (°C)	16.5 ± 2.4	12.3	19.9
SST (°C)	16.8 ± 13.4	13.4	19.5
Ta-SST (°C)	0.15 ± 0.68	-0.9	1.3
Surface Pressure (mb)	1017.4 ± 2.2	1014.4	1022.8
Relative Humidity (%)	81.8 ± 10.8	62.0	99.2
% of MABL that is cloud	40.6 ± 17.3	8.7	69.5
True Wind Speed (m/s)	5.5 ± 3.5	0.9	11.7

Table 9. Composite non-track case environment.

APPENDIX B. FORMULAE AND PROCEDURES

The following description of the formulae and procedures used in processing the sounding data from MAST was provided by Mr. William Syrett of the Pennsylvania State University. Procedures for processing SEAHUNT sounding data are similar with one known exception that will be noted.

Parameters measured by the radiosondes were pressure, temperature and relative humidity, with winds calculated using the Omega network. The "Omega" winds were averaged over a four-minute period by the sounding system software.

Raw temperature and humidity data were output at 1.5 second intervals, with winds output every 10 seconds. The raw temperatures and humidities were averaged to 5-second intervals, while winds were simply interpolated to 5 seconds.

Three sets of interpolated data were created: 5-second, 20-meter and 2-millibar. The 20-meter resolution data was used in this thesis. The SEAHUNT data set used 5-second data.

Derived quantities include height, dewpoint and mixing ratio. The formulae used for mixing ratio, dewpoint and height are (in FORTRAN format):

Mixing Ratio (w):

$$w = 622.0*(e/(p-e))$$

p = pressure (mb)
e = vapor pressure (mb)

where: $e = RH*es/100.00$

RH = relative humidity
es = sat. vapor pres (mb)

where: $es = 6.112*EXP((17.67*T)/(T+243.5))$

T = temperature(deg C)

Height (z):

$$z(i) = z(i-1)+(R*TvA/g)*LN(p(i-1)/(p(i)))$$

R=gas constant (J/kg K)
g = acc. due to gravity

where: TvA is the layer averaged virtual temperature
$Tv = T*(1.0+0.61*w)$; w in g/g, Tv in degrees Kelvin
for height computation

81

Dewpoint:

$$Td = (243.5 * LN(e/6.112))/(17.67 - LN(e/6.112))$$

Relative humidities were adjusted upward, based on both observed cloudiness in relation to reported humidities and also on a conversation between Mr. Syrett with a Vaisala (system manufacturer) employee familiar with the humidity sensor on the RS-80 sondes used at the sites. The adjustment procedure is similar to that used for ASTEX soundings. The adjustment procedure is described in Syrett (1994).

LIST OF REFERENCES

Ackerman, A.S., O.B. Toon, and P.V. Hobbs: Dissipation of marine stratiform clouds and collapse of the marine boundary layer due to the depletion of cloud condensation nuclei by clouds. *Science*, **262**, 226-229.

Albrecht, B.A., 1989: Aerosols, cloud microphysics and fractional cloudiness. *Science*, **245**, 1227-1230.

Albrecht, B.A., D.A. Randall and S. Nicholls, 1988: Observations of marine stratocumulus during FIRE. *Bull. Amer. Meteor. Soc.*, **69**, 618-626.

Bowley, C.J., 1967: Comments on atmospheric requirements for the genesis of anomalous cloud lines. *J. Atmos. Sci.*, **24,** 596-597.

Charlson, R.J., S.E. Schwartz, J.M. Hales, R.D. Cess, J.A. Coakley Jr., J.E. Hansen and D.J. Hofman, 1992: Climate forcing by anthropogenic aerosols. *Science*, **255**, 423-430.

Charlson, R.J., J.E. Lovelock, M.O. Andreae, and S.G. Warren, 1987: Oceanic phytoplankton, atmospheric sulphur, cloud albedo, and climate. *Nature*, **326**, 655-661.

Coakley, J.A. Jr., R.L. Bernstein and P.A. Durkee, 1987: Effect of ship-stack effluents on cloud reflectivity. *Science*, **237**, 1020-1022.

Conover, J.H., 1966: Anomalous Cloud Lines. *J. Atmos. Sci.*, **23**, 778-785.

Durkee, P.A., 1994: *Monterey Area ShipTrack Experiment [CNO Project K-1420] Science Plan.* 42pp.

Evans, M.E., 1992: Analysis of shiptracks in cloudiness transitions regions. M.S. Thesis, Naval Postgraduate School, Monterey, CA, 93pp.

Giampaolo, V., 1992: Shiptrack detection algorithm study. M.S. Thesis, Naval Postgraduate School, Monterey, CA, 97pp.

Hindman, E.E., 1990: Understanding ship-trail clouds. Preprints of 1990 Conference on Cloud Physics, July 23-27, 1990, San Francisco, CA, A.M.S., Boston, MA 1990.

King, M.D., T. Nakajima and L.F. Radke, 1990: Optical properties of marine stratocumulus clouds modified by ship track effluents. Preprints of 1990 Meeting of the American Meteorological Society, San Francisco, CA, 396-400.

Klein, S.A., and D.L. Hartmann, 1993: The seasonal cycle of low stratiform clouds. *J. Climate*, **6**, 1587-1606.

Kuciauskas, A., P.A. Durkee, C. Skupniewicz, and K.E. Nielsen, 1993: Radiative characteristics of shiptracks at night. Presented at Cloud Impacts on DOD Operations and Systems (CIDOS-93), 16-19 November, 1993, Fort Belvoir, VA.

Lilly, D.K., 1968: Models of cloud-topped mixed layers under a strong inversion. *Quart. J. Roy. Meteor. Soc.*, **94**, 292-309.

Lutz, J.W., 1992: A summary of shiptrack effects on clouds over the eastern North Pacific Ocean. M.S. Thesis, Naval Postgraduate School, Monterey, CA, 64pp.

Mays, D., 1993: Shiptrack database analysis. M.S. Thesis, Naval Postgraduate School, Monterey, CA, 60pp.

Millman, T., 1992: A temporal analysis of east Pacific and east Atlantic shiptracks. M.S. Thesis, Naval Postgraduate School, Monterey, CA. 69pp.

Mineart, G.M., 1988: Multispectral satellite analysis of marine stratocumulus cloud microphysics. M.S. Thesis, Naval Postgraduate School, Monterey, CA, 138pp.

Morehead, S.E., 1988: Ship track cloud analysis for the North Pacific area. M.S. Thesis, Naval Postgraduate School, Monterey, CA, 57pp.

Office of Naval Research, 1994: *Monterey Area ShipTrack Experiment [CNO Project K-1420] Operations Plan*, pp. 1.1 - B12.

Pettigrew, J.C., 1992: Surface meteorological parameters of identified shiptracks. M.S. Thesis, Naval Postgraduate School, Monterey, CA, 71pp.

Platnick, S. and S. Twomey, 1994: Determining the susceptibility of cloud albedo to changes in droplet concentration with the advanced very high resolution radiometer. *J. Appl. Meteor.*, **33**, 334-347.

Porch, W.M., C-Y Kao, and R.G. Kelley, 1990: Ship trails and ship induced cloud dynamics. *Atmos. Environ.*, **24A**, 1051-1059.

Porch, W.M., M. Buchwald, T. Glatzmaier, C.-Y. J. Kao, W. Unruh, J. Hudson, F. Rogers, P. Durkee, E. Hindman, and J. Kocian, 1992: Experimental and theoretical investigations of marine stratocumulus cloud sensitivity to climate parameters using ship-trail clouds, Third Symposium on Global Change Studies, Amer. Meteor. Soc., Jan 5-10, 1992, Atlanta, GA.

Porch, W.M., C-Y Kao, M.I. Buckwald, W.P Unruh, P.A. Durkee, E.E. Hindman, and J. G. Hudson, in press: The effects of external forcing on the marine boundary layer: ship trails and a solar eclipse.

Radke, L.F., J.A. Coakley, Jr. and M.D. King, 1989: Direct and remote sensing observations of the effects of ships on clouds. *Science,* **246**, 1146-1149.

Rosenthal, J., and R. Helvey, 1992: *Refractive Assessments from Satellite Observations*, AGARD CP-502, pp. 8.1 - 8.9.

Salvato, G., 1992: Comparison between arctic and subtropic ship exhaust effects on cloud properties. M.S. Thesis, Naval Postgraduate School, Monterey, CA, 56pp.

Stull, R.B., 1988: *An Introduction to Boundary Layer Meteorology*. Kluwer Academic Publishers, Dordrecht. 666pp.

Twomey, S., 1968: On the composition of cloud nuclei in the northeasten United States. *J. Rech. Atmos.*, **3**, 281-285.

INITIAL DISTRIBUTION LIST

No. Copies

1. Defense Technical Information Center 2
   Cameron Station
   Alexandria, Virginia 22304-6145

2. Library, Code 52 2
   Naval Postgraduate School
   Monterey, California 93943-5101

3. Chairman (Code MR/Hy) 1
   Department of Meteorology
   Naval Postgraduate School
   Monterey, California 93943-5002

4. Chairman (Code OC/Bf) 1
   Department of Oceanography
   Naval Postgraduate School
   Monterey, California 93943-5002

5. Professor Philip Durkee (Code MR/De) 1
   Department of Oceanography
   Naval Postgraduate School
   Monterey, California 93943-5002

6. Professor Kenneth Davidson (Code MR/Ds) 1
   Department of Oceanography
   Naval Postgraduate School
   Monterey, California 93943-5002

7. Mr. Bob Bluth 1
   Code 4513 Office of Naval Research
   Room 522
   800 North Quincy St.
   Arlington, Virginia 22217-5000